修士論文の和文要旨

研究科・専攻	大学院情報理工学学研究科 情報・ネットワーク工学専攻　博士前期課程		
氏　　　名	相原 直紀	学籍番号	1831002
論 文 題 目	Machine Learning Aided Orthogonal Resource Allocation In Heterogeneous Low Power Wide Area Networks		

要　　旨

近年，IoT の発展に伴い，長距離通信・超低消費電力・同時多接続などの要件が重要視されている．これらの要求に対応するため，LoRaWAN(Long Range Wide Area Network)に代表される LPWAN(Low Power Wide Area Network)通信規格に注目が集まっている．これらの規格では，無線ノードの低消費電力化のために各レイヤにおいて単純な機能が用いられている．例えば，MAC 層では，集中制御ではなく各無線ノードが自律分散的にランダムアクセスを行うことで周波数リソースの共用を行う多元接続方式が採用されている．このような単純な通信制御では，無線ノード数の増加に伴いパケット衝突が頻発することが大きな問題である．この問題の解決策としては，無線資源を有効に活用できるようなリソース割り当てが挙げられる．しかしながら，LoRaWAN 環境においては，拡散係数 (SF: Spreading Factor)と呼ばれる物理層変調パラメータの割り当てしか行われておらず，システムで利用可能な複数の周波数リソースに関しては，各端末がパケット送信時にランダムに周波数を移動するランダムホッピングが適用されている．更に，既存研究は明示的なフィードバックやチャネル推定に基づくものが大半であり，これらの方式はリソース割り当てのために余剰なオーバーヘッドを必要とする．また，920[MHz]帯での利用を想定した場合には，一つの帯域を特定のシステムが専有することは現実的ではなく，複数のシステムが周波数を共用することになる．例えば，使用帯域が重なる LoRaWAN システムと Wi-SUN システム間での相互干渉の影響が挙げられる．このように，実際には他システムの影響を考慮したリソース割り当てが重要である．

本論文では，衝突機能回避付きキャリアセンス多元接続(CSMA/CA: Carrier Sense Multiple Access/Collision Avoidance)を MAC 層の多元接続方式として用いる LoRaWAN 環境において，強化学習に基づく効率的な周波数リソース割り当て方式を提案する．本提案方式では，各 LoRaWAN ノードから正しく受信できたパケット数という，LoRaWAN の情報集約局(FC: Fusion Center)で観測できる情報のみを用いて強化学習を行うことで，LoRaWAN ノードからの明示的なフィードバックやチャネル推定などの処理を必要とせずに効率的な周波数リソースの割り当てを行うことが可能である．また，これに加えて，密度比推定に基づく分布変化検知を利用した外部からのシステム間干渉の変動に追従できるような干渉検知方式および無線リソース再割当て方式を提案する．計算機シミュレーションにより，提案手法は従来の手法と比較して平均で 13%程度パケット配信率(PDR: Packet Delivery Rate)を向上でき，さらに最大で 3 回程度の観測で外部干渉の状態変化を検知でき，干渉検知を行わない場合と比較して最大で平均 10%程度 PDR を向上できることを示す．

令和元年度　修士論文

Machine Learning Aided Orthogonal Resource Allocation In Heterogeneous Low Power Wide Area Networks
異種LPWAネットワーク混在環境における機械学習を用いた直交リソース割り当て方式

学籍番号	**1831002**
氏名	相原　直紀
情報・ネットワーク工学専攻	情報通信工学プログラム
主任指導教員	安達　宏一 准教授
指導教員	石橋　功至 准教授
提出日	令和**2**年**3**月**16**日

主指導教員印	指導教員印

和文概要

近年，IoT の発展に伴い，長距離通信・超低消費電力・同時多接続などの要件が重要視されている．これらの要求に対応するため，LoRaWAN(Long Range Wide Area Network) に代表される LPWAN(Low Power Wide Area Network) 通信規格に注目が集まっている．これらの規格では，無線ノードの低消費電力化のために各レイヤにおいて単純な機能が用いられている．例えば，MAC 層では，集中制御ではなく各無線ノードが自律分散的にランダムアクセスを行うことで周波数リソースの共用を行う多元接続方式が採用されている．このような単純な通信制御では，無線ノード数の増加に伴いパケット衝突が頻発することが大きな問題である．この問題の解決策としては，無線資源を有効に活用できるようなリソース割り当てが挙げられる．しかしながら，LoRaWAN 環境においては，拡散係数 (SF: Spreading Factor) と呼ばれる物理層変調パラメータの割り当てしか行われておらず，システムで利用可能な複数の周波数リソースに関しては，各端末がパケット送信時にランダムに周波数を移動するランダムホッピングが適用されている．更に，既存研究は明示的なフィードバックやチャネル推定に基づくものが大半であり，これらの方式はリソース割り当てのために余剰なオーバーヘッドを必要とする．また，920[MHz] 帯での利用を想定した場合には，一つの帯域を特定のシステムが専有することは現実的ではなく，複数のシステムが周波数を共用することになる．例えば，使用帯域が重なる LoRaWAN システムと Wi-SUN システム間での相互干渉の影響が挙げられる．このように，実際には他システムの影響を考慮したリソース割り当てが重要である．

本論文では，衝突機能回避付きキャリアセンス多元接続 (CSMA/CA: Carrier Sense Multiple Access/Collision Avoidance) を MAC 層の多元接続方式として用いる LoRaWAN 環境において，強化学習に基づく効率的な周波数リソース割り当て方式を提案する．本提案方式では，各 LoRaWAN ノードから正しく受信できたパケット数という，LoRaWAN の情報集約局 (FC: Fusion Center) で観測できる情報のみを用いて強化学習を行うことで，LoRaWAN ノードからの明示的なフィードバックやチャネル推定などの処理を必要とせずに効率的な周波数リソースの割り当てを行うことが可能である．また，これに加えて，密度比推定に基づく分布変化検知を利用した外部からのシステム間干渉の変動に追従できるような干渉検知方式および無線リソース再割当て方式を提案する．計算機シミュレーションにより，提案手法は従来の手法と比較して平均で 13%程度パケット配信率 (PDR: Packet Delivery Rate) を向上でき，さらに最大で 3 回程度の観測で外部干渉の状態変化を検知でき，干渉検知を行わない場合と比較して最大で平均 10%程度 PDR を向上できることを示す．

Abstract

Recently, a network that satisfies long-range, ultra-low power consumption, and massive connectivity requirements is considered due to the development of Internet of Things (IoT). To deal with these requirements, low power wide area (LPWA) protocol, especially long range wide area network (LoRaWAN) becomes a promising technology. In this protocol, naive functions are used in each layer for low power consumption of wireless nodes. For example, distributed random access schemes are used instead of centralized control schemes as multiple access schemes in the medium access control (MAC) layer. If these naive control schemes are adopted, packet collision frequently happens with an increase in the number of wireless nodes. Some research tackles this problem using efficient resource allocation. However, in LoRaWAN environment, existing researches only consider the allocation of allocate spreading factor (SF) that is a modulation parameter in the physical layer. Therefore, these researches assume random hoping that each terminal hops frequency randomly at the start of transmission of each packet. On the other hand, the assumption that one system takes possession of a frequency band is unrealistic. In a realistic environment, multiple systems share the same frequency bands. Existing research experiments the effect of mutual interference between different systems that is called *cross-technology interference* or *inter-system interference*. Therefore, efficient resource allocation and communication control schemes considering the effects of other system are necessary.

In this research, we propose an efficient resource allocation scheme based on reinforcement learning in a carrier sense multiple access/ collision avoidance (CSMA/ CA) adopted LoRaWAN environment. In the proposed scheme, reinforcement learning is executed using the information of the number of successfully received packets that is observable at a fusion center (FC). By this scheme, efficient resource allocation becomes executable without explicit feedback and channel estimation, and so on. Moreover, we propose an inter-system interference detection scheme using distribution change detection based on density ratio estimation and resource reallocation scheme. By computer simulation, it is shown that the proposed scheme can improve the average packet delivery rate (PDR) performance by about 13% compared to a random hopping scheme, which is currently adopted in the LoRaWAN system. Furthermore, the proposed inter-system interference

detection scheme can detect the change of inter-system interference state within at most 3 observation, and hence can improve the average PDR by about 10% compared to the system without detection scheme.

Contents

Chapter 1

Introduction **1**

1.1 Background 1

1.2 Machine Learning Aided Wireless Communication System 3

1.3 Purpose of Research 3

Chapter 2

LoRaWAN **5**

2.1 Physical Layer 5

2.2 MAC Layer and Multiple Access Scheme 5

Chapter 3

System Model **7**

3.1 System Model 7

3.2 Channel Model 10

3.3 Interference Model 11

3.4 Problem Formulation 11

Chapter 4

Machine Learning Technology **13**

4.1 Q-learning 13

4.1.1 Q-learning Model 13

4.1.2 Q-learning using Neural Network 14

4.2 Neural Network (NN) 14

4.2.1 Forward Propagation 15

4.2.2 Back Propagation 16

4.2.3 Optimizer 18

4.3 Density Ratio Estimation 18

4.3.1 Definition 18
4.3.2 Advantage of Density Ratio Estimation 19
4.3.3 Steps of Optimization of Density Ratio Estimation Model 20
4.3.4 Anomaly Detection and Change Detection 21

Chapter 5

Proposed Scheme **23**

5.1 Q-Learning Aided Resource Allocation 23
5.1.1 Design of Learning Model 23
5.1.2 Resource Allocation using Q-learning 24
5.2 Density Ratio Estimation based Interference Detection and Resource Reallocation 25
5.2.1 Distribution Change Detection using Sliding Window 25
5.2.2 ReLearning 27

Chapter 6

Performance Evaluation **28**

6.1 Performance Evaluation of Q-Learning Aided Resource Allocation 28
6.1.1 Impacts of Learning Parameters 30
6.1.2 PDR Performance 31
6.2 Interference Detection and Resource Reallocation 32
6.2.1 Case 1: Interference Appearance 33
6.2.2 Case 2: Interference Disappearance 33

Chapter 7

Conclusion **40**

Acknowledgments **41**

Publications **47**

Chapter 1

Introduction

1.1 Background

Wireless access technologies have been evolving to meet the demand for high-speed communication. Similarly, low power consumption communication is becoming more important due to the emerge of the Internet-of-Things (IoT) with low communication speed [1]. Long range wide area network (LoRaWAN) is one of the promising network structures for low power wide area (LPWA) networks, which provide low speed, long-range communication for distances of up to 10 km. The chirp spread spectrum (CSS) technique is adopted for the physical layer of LoRaWAN. For the medium access control (MAC) layer, each LoRaWAN node adopts pure ALOHA [2]. Due to this simple MAC protocol, packet collision increases as the number of LoRaWAN nodes increases. This is a critical factor to limit network performance. One of the countermeasures is the introduction of a duty cycle (DC) that limits the channel occupancy ratio of each node to a predetermined threshold [3]. Recently, the application of carrier sense multiple access with collision avoidance (CSMA/CA) has been introduced to improve the performance of LoRaWAN [4, 5]. For example, CSMA/CA is essential for LoRaWAN in Japan [6]. In this protocol, LoRaWAN nodes sense the wireless medium before starting packet transmission. However, due to the wide communication area and the low transmission power of nodes, packet collision happens quite often LoRaWAN in comparison to legacy wireless local area network (WLAN) systems. Because the LoRaWAN node has limited functionality due to its low cost, the introduction of more complicated interference management technologies is not appropriate. In LoRaWAN, there are mainly two parameters that can be used for interference avoidance or rejection, namely, a spreading factor (SF) and a frequency channel. In LoRaWAN, there are 6 SFs are defined. Increasing SF makes the signal transmission more robust against the noise at the cost of the reduced transmission rate. If different SFs are used among different nodes, the interference rejection can be achieved. In LoRaWAN, there are up to 16 orthogonal frequency channels can be used for each system [2]. Currently, at the start of each packet transmission, each LoRaWAN node randomly selects one of the frequency channels assigned by its fusion center (FC). In existing works, SF allocation has been considered in order to avoid packet collision and mitigate mutual interference [7–12]. One potential solution to further improve network performance is to allocate orthogonal frequency channels to LoRaWAN nodes that often collide with each other. However, orthogonal frequency channel allocation is difficult due to the large scale of the network and the limited functionality of LoRaWAN nodes. Moreover, LoRaWAN nodes cannot inform the FC of their surrounding wireless environments, such as how often each LoRaWAN node can carrier sense (CS) the on-going communication due to its limited functionality. Thus, a resource allocation scheme that does not require such feedback from nodes is demanded.

So far, most research works assume that there is only one system in the communication area, i.e., the system of interest can occupy the frequency band exclusively. However, this assumption may not be appropriate in a realistic scenario. Since multiple systems share the same frequency band in a more realistic scenario, the performance of the system may be severely degraded by the inter-system interference. In [13], *inter-system interference* or so called *cross-technology interference (CTI)* between LoRaWAN and wireless-sensor utility network (Wi-SUN) is experimentally evaluated under overlapping operating frequency bands. This CTI disturbs each independent operating system. Therefore, efficient resource allocation and communication control schemes considering the effects of other systems are necessary. To take into account the inter-system interference, it is necessary to detect the inter-system interference state. Up to now, roughly two types of research works have been done to detect the inter-system interference that is introduced by the other system. The first type is based on spectrum sensing [14, 15]. Cognitive radio, using hidden markov model, based interference detection system and a channel sensing based interference change detection system are proposed, respectively in [14] and [15]. However, these researches are based on highly accurate spectrum sensing. Therefore, these schemes may not be suitable for the LPWA system due to low-cost devices. The second type is based on the error pattern of chips, symbols, and packets [16–18]. In [16] the relationship between chip error pattern and channel conditions, such as channel attenuation and interference, is analyzed. In [17], the difference between bit/ symbol error distribution with different interference situation is presented. In [18], *channel analysis signal* that can detect existence of interference signal is proposed and interference classification performance is evaluated. However, these schemes rely on some assumptions about typical interference systems, e.g., the same physical layer technology with the different systems or wireless local area network (WLAN). Therefore, these systems cannot be adopted for arbitrary systems. Moreover, most of the conventional schemes only consider detecting the appearance of inter-system interference. From the viewpoint of operational principles, it is preferable to detect the change of interference state, i.e., the appearance and the disappearance.

1.2 Machine Learning Aided Wireless Communication System

Recently, a machine learning technique for wireless networks becomes a key enabler for such situations. This technique is often used to optimize wireless resource allocation, e.g., transmit power control, frequency allocation, beamforming vector, BS operation, and so on [19–23]. However, a supervised learning technique is difficult to be applied to wireless networks. This is because, in a wireless network environment, harvesting training set, which is the pair of input and output, is usually difficult due to the overhead of feedback. Therefore, especially, deep-Q-network (DQN) [24] and unsupervised learning-based schemes are frequently used to optimize wireless network operation because these technologies do not require training set.

1.3 Purpose of Research

In this thesis, we propose to utilize a powerful machine learning technique for efficient orthogonal channel assignment in LoRaWAN with CSMA/CA. Because it is difficult to obtain the training set in a practical system, we focus on *reinforcement learning*. Reinforcement learning can learn the environment without a training set by observing the output from the environment after its action. To the best of our knowledge, this is the first work that tackles orthogonal resource allocation in LoRaWAN where additional information exchange is not allowed. The number of successfully received packets at an FC is used as the reward of learning so that no explicit feedback from a LoRaWAN node is required. Because there is a strong correlation between the number of received packets and packet delivery rate (PDR), this resource allocation can improve PDR performance. The proposed scheme is shown to improve the average PDR performance by 13% compared to the random allocation scheme through computer simulation with consideration for LoRaWAN specification.

In order for the proposed resource allocation technique to work under the impact of the inter-system interference, an interference state change detection is developed for further utilization of resources. Since the appearance and the disappearance of the inter-system interference change the state, the proposed scheme enables more efficient resource utilization. For the interference state change detection, a density ratio estimation [25] is applied. In order not for requiring training data, pseudo training data and test data are generated. Those data are obtained by sequentially generating a set of the sample values on each frequency channel. By this, the change of the inter-system interference state can be detected without any prior knowledge. Once the change of the inter-system interference state is detected, the frequency channel is reassigned to LoRaWAN nodes by relearning. The performance improvement brought by the proposed detection scheme is confirmed by computer simulation assuming the coexistence of LoRaWAN and Wi-SUN. It is shown that the average packet delivery rate (PDR) can be improved by about 10% by introducing the proposed inter-system interference state change detection and relearning.

The rest of this thesis is organized as follows. In Sect. 2, the basic functions and features of LoRaWAN system are introduced. In Sect. 4, the existing learning schemes are briefly reviewed. In Sect. 3, the system model concisdered in this thesis is introduced. The proposed Q-learning based wireless resource allocation and inter-system interference detection system are presented in Sect. 5. In Sect. 6 provides computer simulation results. Sect. 7 concludes the thesis.

Chapter 2

LoRaWAN

2.1 Physical Layer

LoRaWAN is one of the LPWA standards. LoRaWAN adopts CSS modulation as a physical layer technology. Its data rate and communication range are determined by SF. The value of SF determines the communication distance. With a higher SF, the receiver can receive packets with lower received signal power, at the cost of the reduced data rate. Let the frequency bandwidth denoted by W [Hz]. Then, a chip length T_c [sec] of the CSS symbol is given by $T_\mathrm{c} = \dfrac{1}{W}$ [sec]. The CSS symbol length T_s [sec] is given by

$$T_\mathrm{s} = T_\mathrm{c} \times 2^{SF}, \tag{2.1}$$

where SF denotes the value of SF. As SF increases, the transmitted signal has stronger resistance against noise and interference at the expense of the data rate. The typical data rate and signal-to-noise power ratio (SNR) limit are shown in Table 2.1.

The CSS modulated signal is transmitted over one of the orthogonal frequency channels. For LoRaWAN, there are up to K orthogonal frequency channels that depend on region and frequency [26]. Each FC can inform the available channel indices to each LoRaWAN node. [2].

2.2 MAC Layer and Multiple Access Scheme

Three classes are defined for LoRaWAN nodes, i.e., class A, B, and C [2]. Class A is mandatory for all LoRaWAN nodes. Class A nodes receive the downlink transmission together with an acknowledgment (ACK) message via two receive windows that are open after the uplink transmission of a node. Class B nodes periodically open a beacon receive window. Class C nodes always open a receive window in order

Table 2.1: Data rate and SNR limit

SF	Data rate [bps]	Receiver sensitivity [dBm] [27]	SNR limit [dB]
7	5469	-123	-6
8	3125	-126	-9
9	1758	-129	-12.5
10	977	-132	-15.0
11	537	-134.5	-17.5
12	293	-137	-20.0

to receive a message from the FC. Thus, an FC can inform each node of necessary commands such as available frequency channels via downlink transmission.

In the LoRaWAN standardization, the implementation of pure ALOHA protocol is mandatory as a MAC layer in LoRaWAN as its simple operation is suitable for low-cost LoRaWAN nodes. However, recently, the adaptation of CSMA/CA is proposed for further performance improvement. For low control overhead, an asynchronous distributed multiple access scheme is needed. Both pure ALOHA and CSMA/CA satisfy this requirement.

Chapter 3

System Model

3.1 System Model

Fig. 3.1 shows the LoRaWAN system considered in this thesis. N LoRaWAN nodes are randomly and uniformly distributed within a network area of $D \times D$ [km^2]. One FC that controls LoRaWAN nodes and receives information from them is located at the center of the area. In total, K orthogonal frequency channels are available in this system. Let us denote the set of LoRaWAN nodes and that of the orthogonal frequency channels as $\mathcal{N}$ and $\mathcal{K}$, respectively. For LoRaWAN, there are up to K orthogonal frequency channels. The number of available frequency channels depends on region and frequency [26]. Each FC informs the LoRaWAN nodes of the available channel indices [2]. The CSS modulated signal is transmitted from each LoRaWAN node on one of the orthogonal frequency channels.

The second traffic is generated when an event is detected. In this letter, an event occurs once at random time in each epoch at a random position, and it propagates in the communication area with predetermined speed [28]. The exponential propagation model is considered in this letter. In this letter, we assume these traffic type has the same packet size N_{trans} [bits].

Each LoRaWAN node generates traffic of two types [28]. The first traffic is generated regularly at each LoRaWAN node following predetermined packet generation interval $T_{\text{interval},n}$, which is selected from the set $\mathcal{T}_{\text{interval}}$. In this study, the LoRaWAN nodes that have the same packet generation intervals are called *cluster*. A random offset $T_{\text{offset},n} \sim \mathcal{U}[0, T_{\text{interval},n})$ is assigned to LoRaWAN node n, where $\mathcal{U}[X, Y)$ is uniform distribution between X and Y. The packet generation interval indicates the application type in the communication area such as gas meter and water supply meter. Note that even the LoRaWAN nodes with the same packet generation interval may not transmit the packets simultaneously owing to the different offsets. We assume that there are U application types. Thus, on an average, (N/U) LoRaWAN nodes generate packets with the same interval and attempt to send the packet to the FC. The second traffic is generated when an event is detected. In this thesis, an event (e.g., fire and electricity

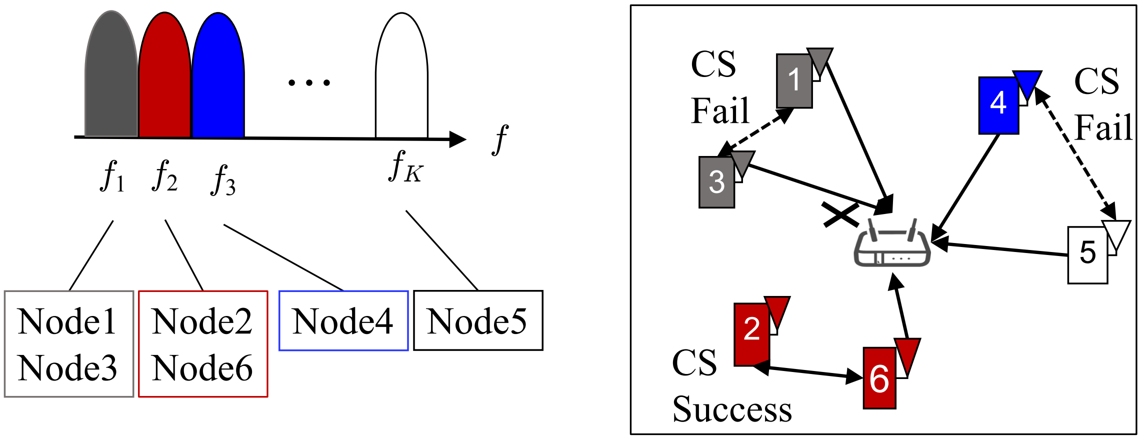

Figure 3.1: System model.

accident) occurs once at random time in each epoch at a random position, and it propagates in the communication area with predetermined speed [28]. The exponential propagation model is considered in this thesis. In this propagation model, each node generates an event packet with probability s_n that is given as

$$s_n = e^{-\alpha \times d_n}, \tag{3.1}$$

where α is an event propagation coefficient and d_n is the distance between LoRaWAN node n and the event center. The example of regular packet generation and the example of event packet generation are shown in Fig. 3.2 and Fig. 3.3. In this thesis, we assume these traffic types have the same packet size N_{trans} [bits].

Each LoRaWAN node transmits packets in accordance with its duty cycle. After finishing a transmission of packet i, LoRaWAN node n waits for the transmission of packet $(i+1)$ for $T_{\text{wait},n,i}$, which is given by

$$T_{\text{wait},n,i} = \frac{1-G}{G} \times \left(\lceil (N_{\text{trans},n,i}/R_b) \rceil \times T_s \right), \tag{3.2}$$

where $N_{\text{trans},n,i}$ is the transmitted packet size of packet i from node n, R_b is the data rate, and $G \in (0, 1]$ is the duty cycle. In this thesis, we assume all packets have the same packet size, i.e., $N_{\text{trans},n,i} = N_{\text{trans}}$. Since LoRaWAN nodes adopt CSMA/CA, each LoRaWAN node waits transmission of its packet until selected *random backoff length*. This backoff length is calculated by uniform distribution with [0,CW], where CW is given as

$$CW = (\text{CW}_{\text{min}} + 1) \times 2^{N_{\text{r},n}} - 1 \tag{3.3}$$

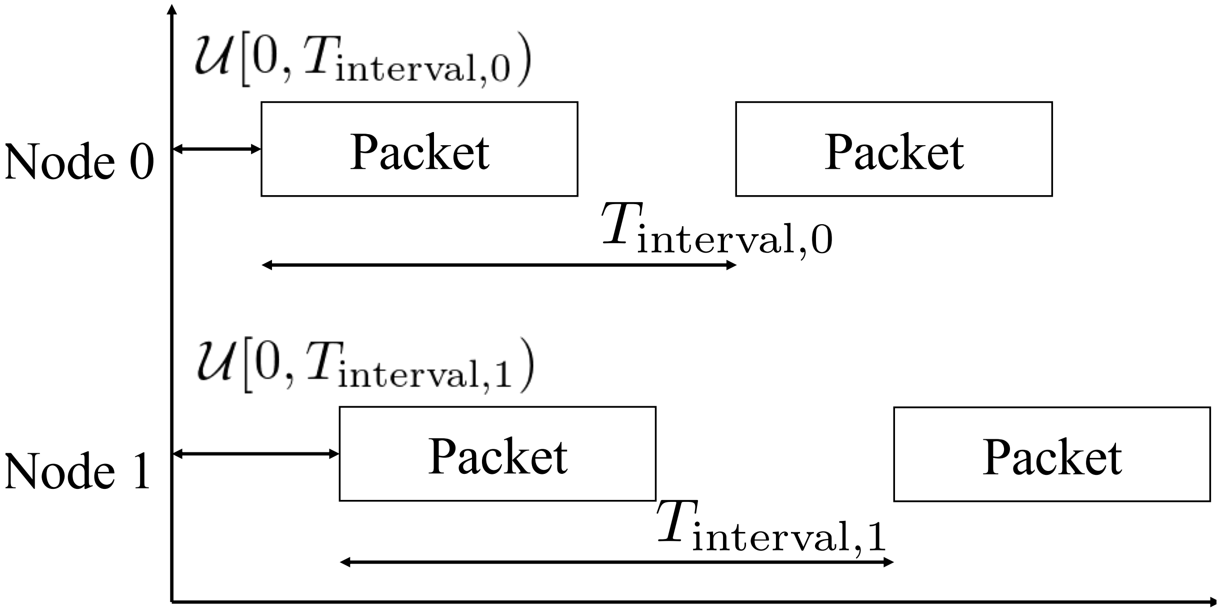

Figure 3.2: regular Packet generation example.

where $\mathrm{CW}_{\min}$ is the minimum backoff length, and $N_{\mathrm{r},n}$ is the number of retransmissions of LoRaWAN node n.

LoRaWAN node n transmits packets with SF $S_n \in \{7, 8, 9, 10, 11, 12\}$. Each SF has its own data rate, signal-to-noise power ratio (SNR) threshold $\Gamma_{\mathrm{SNR},S_n}$, and signal-to-interference power ratio (SIR) threshold $\Gamma_{\mathrm{SIR},S_n}$. In this thesis, we consider a minimum SNR criterion for SF allocation. In this allocation scheme, FC allocates the SF that can maximize data rate while satisfying SNR threshold. If both SNR $\gamma_{\mathrm{SNR},n}$ and SIR $\gamma_{\mathrm{SIR},S_n}$ is above thresholds $\Gamma_{\mathrm{SNR},S_n}$ and $\Gamma_{\mathrm{SIR},S_n}$, the packet from LoRaWAN node n is considered to be successfully received by the FC. For SIR threshold calculation, three thresholds are taken into account as

$$\Gamma_{\mathrm{SIR},S_n} = \max(\Gamma_{\mathrm{co}}, \Gamma_{\mathrm{system},}\Gamma_{\mathrm{inter}}), \tag{3.4}$$

where max(·) is returns the maximum value of the arguments.

- Co-SF Interference Γ_{co}: If there are nodes using the same SF as desired LoRaWAN node n, this interference needs to be considered. The SIR threshold Γ_{SF} is 6 [dB] [29].

- Inter-SF Interference Γ_{inter}: If Wi-SUN interference exists, SIR threshold Γ_{inter} is selected from middle column entitled “w/ Wi-SUN” in Table 2.1.

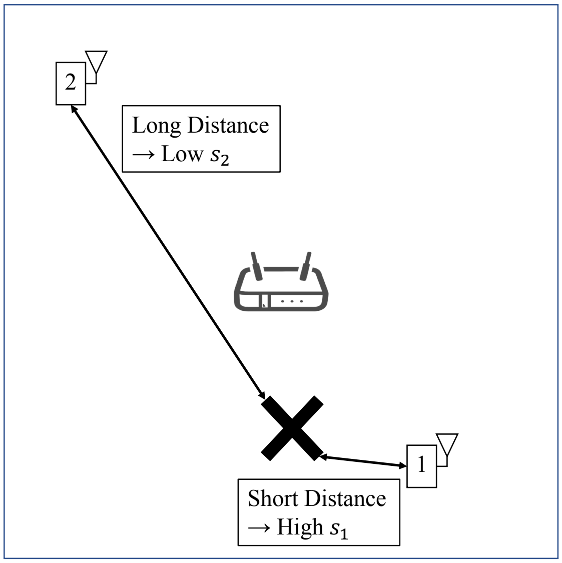

Figure 3.3: Event packet generation example.

- Wi-SUN Interference Γ_{system}: If neither intra-SF interference nor Wi-SUN interference exists, SIR threshold Γ_{intra} is selected from the right column entitled "w/o Wi-SUN" in Table 2.1.

3.2 Channel Model

The received signal power of LoRaWAN node n at the FC is given as

$$P_{\text{r},n}\,[\text{dBm}] = P_{\text{t},n}\,[\text{dBm}] - P_{\text{pl}}(d_n)\,[\text{dB}] - \psi\,[\text{dB}], \tag{3.5}$$

Table 3.1: SIR threshold

SF	SIR threshold [dB] (w/o Wi-SUN interference) [30]	SIR threshold [dB] (w/o Wi-SUN interference) [13]
7	-11.0	-6.0
8	-13.0	-9.0
9	-16.0	-12.5
10	-19.0	-16.0
11	-22.0	-16.0
12	-24.0	-16.0

where $P_{\mathrm{t},n}$ is transmit power of LoRaWAN node n, $P_{\mathrm{pl}}(d_n)$ is a path loss component, ψ is shadowing component that is a function of location of LoRaWAN node (x_n, y_n). The pathloss is given as

$$P_{\mathrm{pl}}(d_n) = 10a\log_{10}d_n + b + 10c\log_{10}f_{\mathrm{c}}, \tag{3.6}$$

where d_n is the distance between LoRaWAN node n and the FC [km], and f_{c} is the carrier frequency [MHz]. Propagation parameters a, b, and c are the coefficients for distance, offset, and frequency loss component, respectively.

3.3 Interference Model

The SNR and SIR for LoRaWAN node n are calculated as

$$\begin{cases} \gamma_{\mathrm{SNR},n} &= \frac{P_{\mathrm{r},n}}{A_{\mathrm{noise}}P_{\mathrm{noise}}} \\ \gamma_{\mathrm{SIR},n} &= \frac{P_{\mathrm{r},n}}{\sum_{n' \in \overline{N}(n)} P_{\mathrm{r},n'} + P_{\mathrm{int},k_{t,n}}}. \end{cases} \tag{3.7}$$

In SNR calculation, A_{noise} is the noise figure and P_{noise} is the noise power. In SIR calculation, the first term of the denominator indicates the intra-system interference that is the sum of received power at FC of interfering LoRaWAN nodes. $\overline{N}(n)$ is the set of interfering LoRaWAN nodes that transmit packets using the same frequency channel with LoRaWAN node n simultaneously. The second term of the denominator indicates the inter-system interference. In this leter, we assume that Wi-SUN flips state $\{$appear, disappear$\}$ at the state change time T_{int}. If Wi-SUN's state is "appear", Wi-SUN packets interfere with LoRaWAN packets with power $P_{\mathrm{int},k}$. We assume that $P_{\mathrm{int},k}$ follows an i.i.d log-normally distribution, i.e., $P_{\mathrm{int},k} \sim e^{\mathcal{N}(\mu_k, \sigma_{\mathrm{int}})}$. Distribution parameters $(\mu_k, \sigma_{\mathrm{int}})$ are obtained from simulation of Wi-SUN nodes received power with transmit power is 13 $[\mathrm{dBm}]$.

3.4 Problem Formulation

Let us denote the PDR of LoWaWAN node n by P_n^{del}, which is given by

$$P_n^{\mathrm{del}} = \frac{R_n}{S_n}, \tag{3.8}$$

where R_n denotes the number of successfully received packets from LoRaWAN node n while S_n denotes the number of packets generated during a predetermined time length T_{epoch}, which is defined as an *epoch*.

The optimal channel selection aims to choose a proper channel to maximize the expected PDR of each node, i.e.,

$$k_n^\star = \underset{k_n \in \mathcal{K}}{\arg\max}\, \mathbb{E}\left[P_n^{\mathrm{del}}\right], \tag{3.9}$$

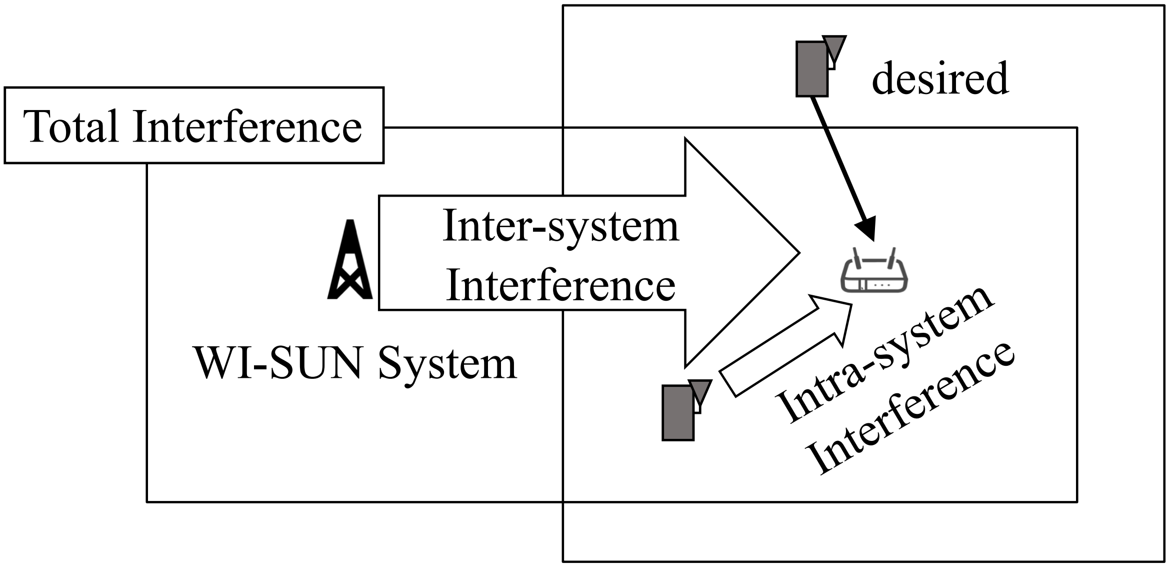

Figure 3.4: Interference model.

where $\mathbb{E}[\cdot]$ denotes the ensemble average operation.

In this thesis, channel allocation is executed every epoch. In this model, R_n depends on the channel allocation of other nodes due to their interference. This makes the optimization problem one of combinatorial optimization problems, i.e., it cannot be solved in practical time. Moreover, S_n also depends on other system parameters. For example, a large T_{wait}, i.e., small duty cycle G, makes the number of transmitted packets small. Thus, the number of successfully received packets becomes small. However, interference also becomes smaller as network traffic is reduced. This phenomenon also happens in the case of large CW.

At FC, it is not possible to know S_n without explicit feedback from LoRaWAN node n. To solve this problem, we propose reinforcement learning-based optimization and approximation of the objective function using only the number of successfully received packets.

Chapter 4

Machine Learning Technology

4.1 Q-learning

Reinforcement learning is one of the learning schemes that search for the optimal action from a given situation. The definition of each terminology that will be used in the following is given below.

Agent an entity that decides the action for a given state.

State information that indicates current environment.

Action impact that Agent can affect to the environment.

Reward evaluation value to agent depend on typical pair of state and action.

Environment the set of {State, Action, Reward}.

The agent is not given the pair of the specific situation with the optimal action. However, the agent is given the reward for a specific situation and an action taken. The agent executes the optimal action based on a reward function that is the sum of the reward of each action. However, this reward function depends on the environment, and it is difficult to solve this function theoretically. To tackle this, the agent approximates the reward function from a taken action and a given reward. This learning scheme is efficient for the specific situations where actions affect subsequent situations, or for situations which provide results from a series of actions, e.g., Markov chain.

4.1.1 Q-learning Model

Let $\mathcal{S}$ and $\mathcal{A}$ be a state set and an action set, respectively. Then, the reward function at time t is approximated by the following update equation:

$$Q(S_t, A_t) \leftarrow Q(S_t, A_t) + \alpha \left[R_{t+1} + \gamma \mathrm{max}_{a \in \mathcal{A}} Q(S_{t+1}, a) - Q(S_t, A_t)\right], \tag{4.1}$$

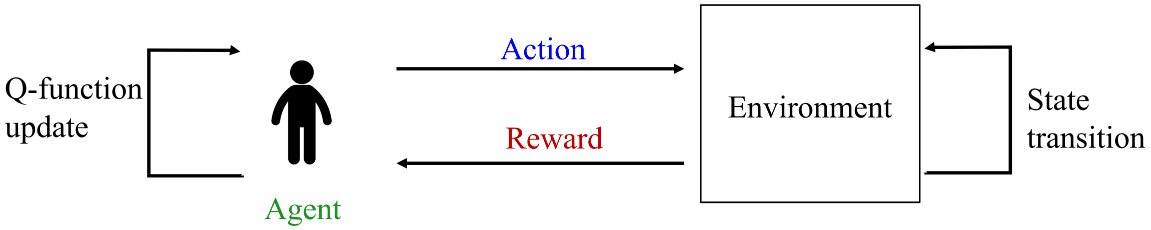

Figure 4.1: Processing flow of Q-Learning.

where $Q(S_t, A_t)$ is the expected value of a reward when an agent takes action $A_t \in \mathcal{A}$ at state $S_t \in \mathcal{S}$. R_{t+1} is an instant reward at time $t+1$ of action A_t, $\gamma \in [0,1]$ is a discount rate, and $\alpha \in (0,1]$ is a Q-learning rate. This approximation converges to real reward function ($Q^{\star}$) [31]. We show the flow of Q-learning in Fig. 4.1.

4.1.2 Q-learning using Neural Network

In traditional Q-learning, the agent needs to keep the Q values for each pair of state and action by using Eq. (4.1); therefore, the agent keeps it as a table of state and action because the Q-value is calculated for each combination of state and action. This format requires an enormous memory capacity when the number of combinations of state and action, ($|\mathcal{S}| \times |\mathcal{A}|$), is large where $|\mathcal{X}|$ is the cardinality of set $\mathcal{X}$. For example, $|\mathcal{S}|$ exponentially increases because it is expressed by the combination of resources allocated to each LoRaWAN node, i.e., $|\mathcal{S}| = |\mathcal{K}|^{|\mathcal{N}|}$ and $|\mathcal{A}|$ linearly increases with the number of available frequency channels, i.e., $|\mathcal{A}| = |\mathcal{K}|$. To avoid such a large memory capacity requirement, a deep-Q-network has been proposed to approximate Q values by a neural network (NN) [24]. An agent can get the approximate model for input and output functions by giving pairs of input and output to NN. By using this, NN learns the weights to output a Q-value approximation for each action $A_t \in \mathcal{A}$ from the input of the current state $S_t \in \mathcal{S}$, as shown in Fig. 4.2.

4.2 Neural Network (NN)

NN is one of machine-learning schemes that approximate the relationship between input and output information by appropriately weighting the connection between *neurons* [32]. NN is composed of two steps: *forward propagation* and *back propagation*, as shown in Fig.4.3. In this thesis, the FC is assumed to have one NN for each of N LoRaWAN nodes, i.e., N NNs in total. In this section, without loss of generality, we review the NN function of node n.

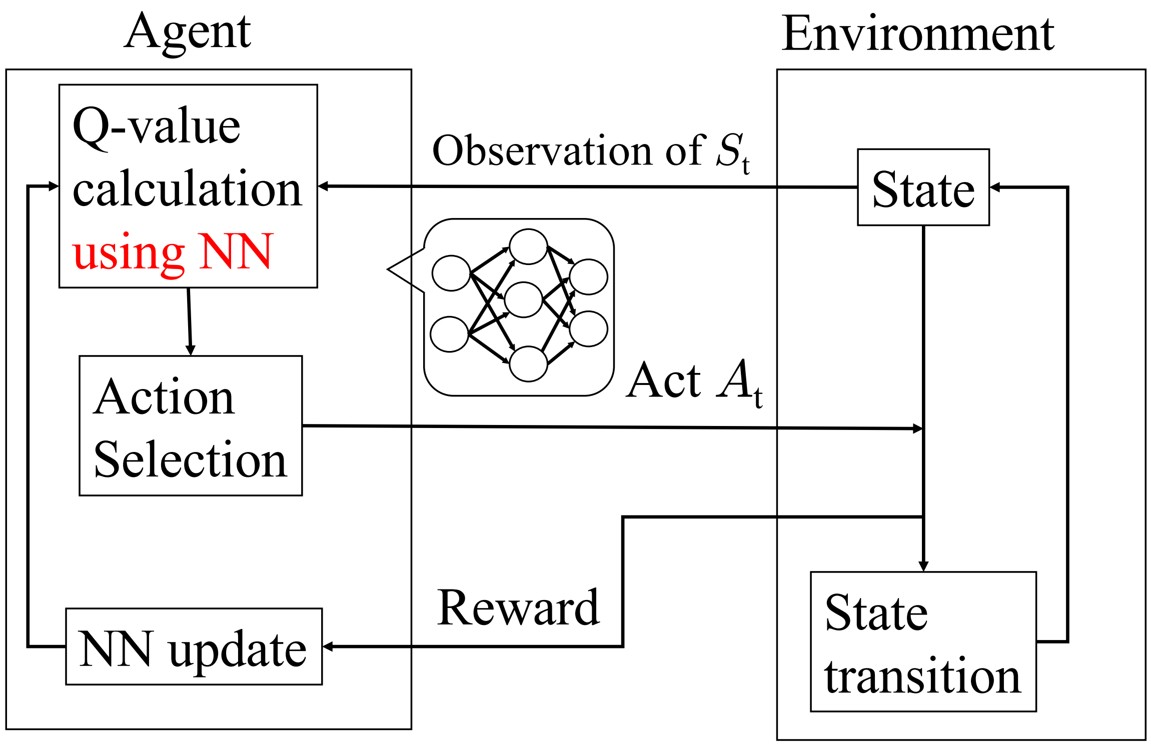

Figure 4.2: Model of Q-learning based on NN.

4.2.1 Forward Propagation

NN is composed of neurons and couplings. Each neuron is arranged hierarchically, and has two functions: *reception* and *activation*, as shown in Fig. 4.4. First, each neuron receives the weighted sum of output from the previous layer. Then, the neuron transforms it by an activation function that is generally nonlinear. Neuron j of layer l receives the weighted sum from the output of neurons in layer $l-1$ as

$$a_{n,j}^{(l)}\left(\mathbf{z}_n^{(l-1)}, \mathbf{w}_{n,j}^{(l-1)}\right) = \sum_i w_{n,i,j}^{(l-1)} \phi(z_{n,i}^{(l-1)}), \tag{4.2}$$

where $w_{n,i,j}^{(l-1)}$ is the coupling weight from neuron i of layer $l-1$ to neuron j of layer l, $z_{n,i}^{(l-1)}$ is the output of neuron i in layer $l-1$, and $\phi(x)$ is a kernel function. For the kernel function, an ideal function is applied as

$$\phi(x) = x. \tag{4.3}$$

Then, neuron j in hidden layer l calculates output $z_{n,j}^{(l)}$ by applying an activation function to $z_{n,j}^{(l)}$ as

$$z_{n,j}^{(l)}\left(\mathbf{z}_n^{(l-1)}, \mathbf{w}_{n,j}^{(l-1)}\right) = f(a_{n,j}^{(l)}), \tag{4.4}$$

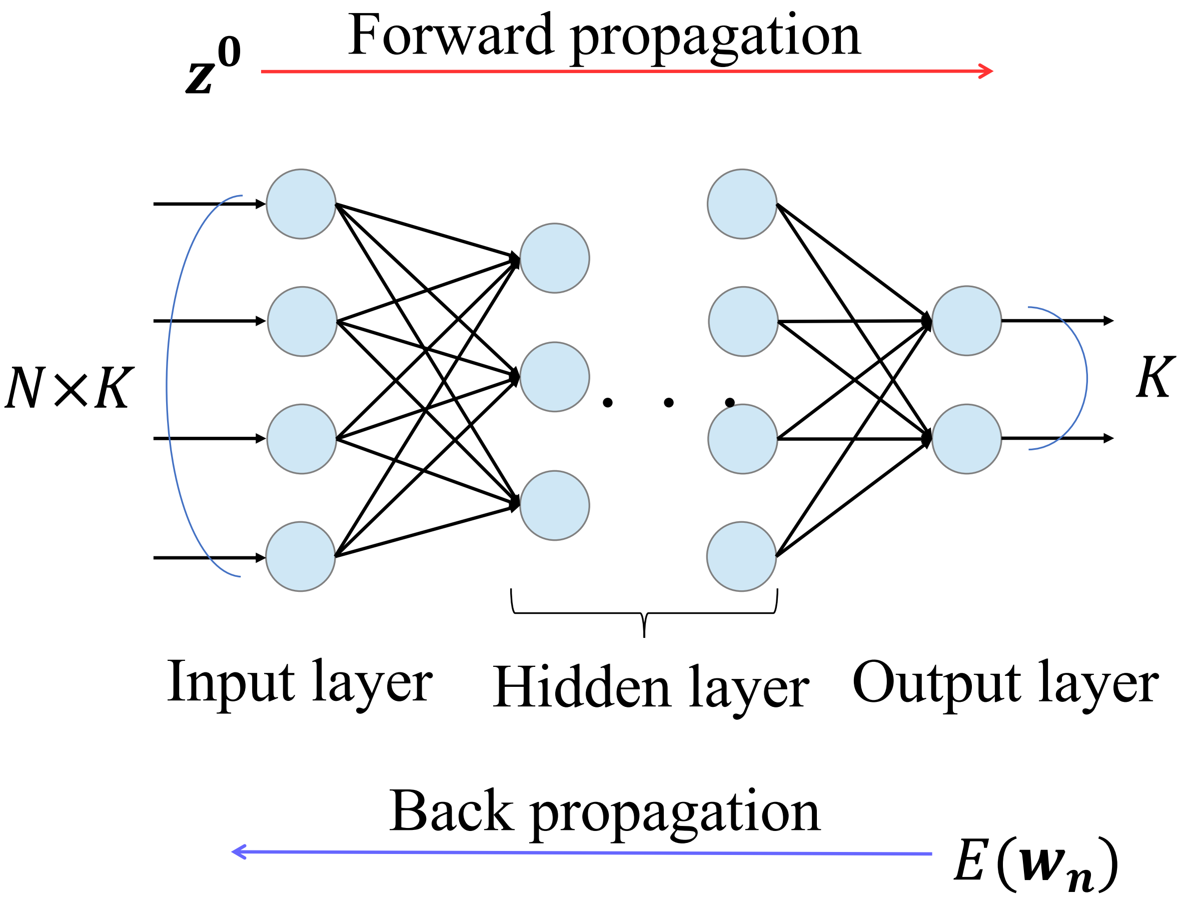

Figure 4.3: Forward propagation and back propagation.

where $f(\cdot)$ is the activation function. Generally, a rectified linear unit (ReLU) function is used for the activation function, which is given as

$$f_{\text{ReLU}}(x) = \max(0, x). \tag{4.5}$$

4.2.2 Back Propagation

The NN weights, $\mathbf{w}_n = \{w^l_{n,i,j}\}$, are trained by using the error function between the output from the NN and the desired output. Let the error function for given NN weights $\mathbf{w}_n$ be $E(\mathbf{w}_n)$. Then, the optimal NN weights, $\mathbf{w}_{n,\text{opt}}$, satisfy

$$\nabla E(\mathbf{w}_{n,\text{opt}}) = 0, \tag{4.6}$$

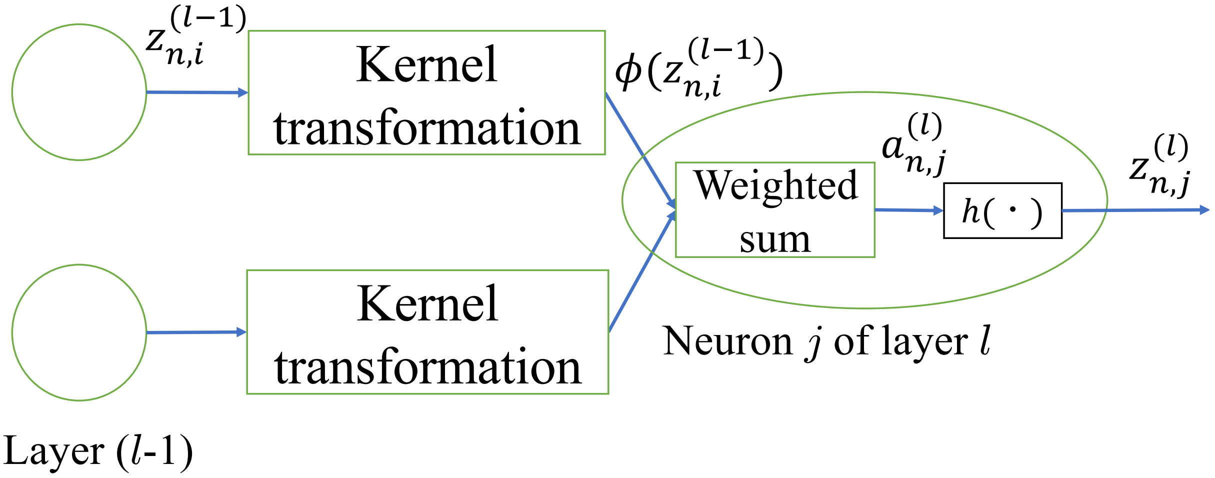

Figure 4.4: Calculation model of NN.

where ∇ is a gradient operator. However, since it is hard to derive the optimal weights analytically, it is common to derive it numerically. The NN parameters are updated from learning time τ as

$$\mathbf{w}_n^{\tau+1} = \mathbf{w}_n^{\tau} - \Delta_n^{\tau}, \tag{4.7}$$

where Δ_n^{τ} is an update term at τ , and initial weights $\mathbf{w}_n^0$ are calculated using some initialization scheme such as Xavier initialization [33].

There are many schemes that calculate update term Δ_n^{τ}, such as stochastic gradient descent (SGD) [32], etc. The gradient value of each coupling weight, $\frac{\partial E_n}{\partial w_{n,i,j}^{(l)}}$, is required to calculate Δ_n^{τ}. *Back Propagation* (BP) is an efficient scheme to calculate the gradient. Without loss of generality, let us focus on the update of weight $w_{n,i,j}^{(l)}$. The gradient is calculated as

$$\frac{\partial E_n}{\partial w_{n,i,j}^{(l)}} \leftarrow \delta_{n,l,j} z_{n,i}^{(l)}, \tag{4.8}$$

where $\delta_{n,l,i}$ is called the *error gradient* that is expressed as

$$\delta_{n,l,j} = \begin{cases} \dfrac{\partial E_n}{\partial z_{n,j}^{(l+1)}} \dfrac{\partial z_{n,j}^{(l+1)}}{\partial a_{n,j}^{(l+1)}} & \text{if } l = L-2 \\ \dfrac{\partial f(a_{n,j}^{(l+1)})}{\partial a_{n,j}^{(l+1)}} \sum_k w_{n,j,k}^{(l+2)} \delta_{n,k}^{(l+1)} & \text{otherwise,} \end{cases} \tag{4.9}$$

where L is the number of layers of NN. In this thesis, a squared error is adopted as the error function $E(\mathbf{w})$, which is given by

$$E(\mathbf{w}_n) = \frac{1}{2}\left(o_{n,k} - z_{n,k}^{(L-1)}\right)^2, \tag{4.10}$$

where $o_{n,k}$ is the training data, and $z_{n,k}^{(L-1)}$ is the approximation of the training data with output k. In this thesis, we want to approximate Q-function, i.e., $o_{n,k} = Q_{n,k_n}$, where Q_{n,k_n} is the actual Q-reward when resource k_n is allocated to LoRaWAN node n.

4.2.3 Optimizer

NN parameter $\mathbf{w}$ is updated as given by Eq. (4.7) using the gradient value as described above. In this thesis, for calculating Δ_n^τ, we use SGD optimizer. In SGD, the gradient value is directly used to calculate and update Δ_n^τ. Although SGD can avoid to stack at a local optimal point, its convergence speed is slow.

For NN, a pure perceptron with L layers is adopted in this thesis. Let us define layer 0 as the input layer and layer $(L-1)$ as the output layer, and the other layers are defined as hidden layers. The update equation for NN weights depends on the optimizer. Let us describe the weight update between neuron i of layer l and neuron j of layer $l+1$ for LoRaWAN node n. In SGD, weight $w_{n,i,j}^{(l)}$ is updated by

$$w_{n,i,j}^{(l)} \leftarrow w_{n,i,j}^{(l)} + \eta \times \frac{\partial E_n}{\partial w_{n,i,j}^{(l)}}, \tag{4.11}$$

where η is an NN learning rate.

4.3 Density Ratio Estimation

Density ratio estimation is one of the machine-learning-based techniques for anomaly data detection [25]. This technique first estimates the ratio of the two distribution and then calculates the abnormality value. If the abnormality value is above a threshold, tested data is considered as abnormal data.

4.3.1 Definition

In this section, we describe the definition of functions and parameters that are needed for this density ratio estimation.

- Baseline distribution $p(\mathbf{x})$: baseline of anomaly detection. Abnormality is calculated by comparing the test distribution that are described below with this baseline distribution.

- Baseline sample $\mathbf{x}_1, \mathbf{x}_2 \cdots, \mathbf{x}_M$: sample vectors from baseline distribution $p(\mathbf{x})$.

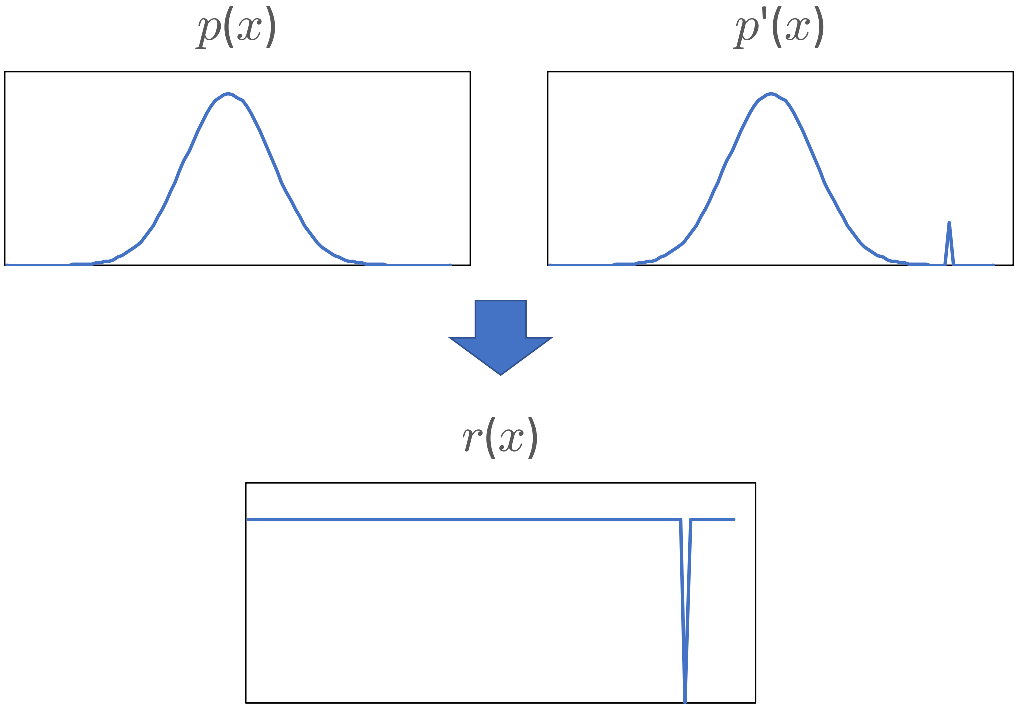

Figure 4.5: Example of density ratio.

- Test distribution $p'(\mathbf{x})$: compared distribution. In this thesis, we assume that abnormal data may be in this distribution.
- Test sample $\mathbf{x'}_1, \mathbf{x}'_2 \cdots, \mathbf{x}'_{M'}$: samples from test distribution $p'(\mathbf{x})$.
- Density ratio $r(\mathbf{x})$: the ratio of two distributions, i.e., $r(\mathbf{x}) = \dfrac{p(\mathbf{x})}{p'(\mathbf{x})}$. If two distribution are the same, this ratio always equals to 1 with any $\mathbf{x}$.
- Abnormality value $a(\mathbf{x})$: output of anomaly detection $a(\mathbf{x}) = -\ln(r(\mathbf{x}))$. If the difference of two distribution is larger (i.e., the density ratio is smaller), this abnormality value becomes larger.

4.3.2 Advantage of Density Ratio Estimation

In this subsection, the reason why a learning model is adopted to calculate the density ratio will be described. Adopting the learning model makes the detection more robust against the estimation error of distributions. Suppose that each distribution is estimated from sample data, the estimation error may affects the result of anomaly detection. This is because estimated $p(\mathbf{x})$ is divided by estimated $p'(\mathbf{x})$. If the estimation error of $p(\mathbf{x})$, that is $\Delta p(\mathbf{x})$ is 0.1 and estimated value of $p'(\mathbf{x})$ is 0.0001, the error of output value $\Delta r(\mathbf{x})$ becomes $\dfrac{10^{-1}}{10^{-4}} = 1000$. Because probability density function is generally smaller than 1 in domain of $\mathbf{x}$, this amplification of estimated density ratio frequently happens. Therefore, generally, density ratio is calculated by learning model $r_{\boldsymbol{\theta}}(\mathbf{x})$, where $\boldsymbol{\theta}$ is learning parameter that is described below.

4.3.3 Steps of Optimization of Density Ratio Estimation Model

The density ratio estimation is composed of the following two steps:

1. Definition of learning model

2. Minimum mean square error (MMSE) based weighting vector optimization from obtained data

Definition of Learning Model

A density ratio is generally modeled as

$$\begin{aligned} r_{\boldsymbol{\theta}(\mathbf{x})} &= \sum_{j=1}^{M} \theta_j \phi_j(\mathbf{x}) && (4.12) \\ &= \boldsymbol{\theta}^T \boldsymbol{\phi}(\mathbf{x}), && (4.13) \end{aligned}$$

where $\boldsymbol{\theta} = (\theta_1, \theta_2 \ldots \theta_M)^T$ is an $M \times 1$ weighting vector, $\boldsymbol{\phi}(\mathbf{x}) = (\phi_1(\mathbf{x}), \phi_2(\mathbf{x}) \ldots \phi_M(\mathbf{x}))^T$ is an $M \times 1$ kernel function vector.

MMSE Based Weighting Vector Optimization from Obtained Data

The purpose of this optimization is to get a learning model $r_{\boldsymbol{\theta}}(\mathbf{x})$ that can provide good approximation of density ratio $r(\mathbf{x})$. Therefore, the optimum weighting vector $\boldsymbol{\theta}_{\mathrm{opt}}$, minimizes the mean squared error (MSE), which is given by

$$\begin{aligned} J(\boldsymbol{\theta}) &= \frac{1}{2}\,\mathbf{E}((r_{\boldsymbol{\theta}(\mathbf{x})} - r(\mathbf{x}))^2) \\ &= \frac{1}{2}\int \{r_{\boldsymbol{\theta}}(\mathbf{x}) - r(\mathbf{x})\}^2 p'(\mathbf{x})\mathrm{d}\mathbf{x} && (4.14) \\ &= \frac{1}{2}\int \{r_{\boldsymbol{\theta}}(\mathbf{x})^2 p'(\mathbf{x}) - 2r_{\boldsymbol{\theta}}(\mathbf{x}) r(\mathbf{x}) p'(\mathbf{x}) + r(\mathbf{x})^2 p'(\mathbf{x})\}\mathrm{d}\mathbf{x}. \end{aligned}$$

Since $r(\mathbf{x})p'(\mathbf{x}) = p(\mathbf{x})$ and $r(\mathbf{x})^2 p'(\mathbf{x})$ is independent of $\boldsymbol{\theta}$, we have

$$\begin{aligned} J(\boldsymbol{\theta}) &= \frac{1}{2}\int \{r_{\boldsymbol{\theta}}(\mathbf{x})^2 p'(\mathbf{x})\}\mathrm{d}\mathbf{x} - \int \{r_{\boldsymbol{\theta}}(\mathbf{x})p(\mathbf{x})\}\mathrm{d}\mathbf{x} + \text{Const} \\ &= \frac{1}{2}\int \{\boldsymbol{\theta}^T \boldsymbol{\phi}(\mathbf{x})\boldsymbol{\phi}(\mathbf{x})^T \boldsymbol{\theta} p'(\mathbf{x})\}\mathrm{d}\mathbf{x} - \int \{\boldsymbol{\theta}\boldsymbol{\phi}(\mathbf{x})p(\mathbf{x})\}\mathrm{d}\mathbf{x} + \text{Const} \\ &= \frac{1}{2}\boldsymbol{\theta}^T \underbrace{\int \{\boldsymbol{\phi}(\mathbf{x})\boldsymbol{\phi}(\mathbf{x})^T p'(\mathbf{x})\}\mathrm{d}\mathbf{x}}_{\triangleq \hat{\mathbf{G}}}\, \boldsymbol{\theta} - \boldsymbol{\theta}^T \underbrace{\int \{\boldsymbol{\phi}(\mathbf{x})p(\mathbf{x})\}\mathrm{d}\mathbf{x}}_{\triangleq \hat{\mathbf{h}}} + \text{Const.} \end{aligned} \tag{4.15}$$

By replacing each expectation operation by the sample average, we have

$$\begin{cases} \hat{\mathbf{G}} = \dfrac{1}{M'}\displaystyle\sum_{m'=1}^{M'} \boldsymbol{\phi}(\mathbf{x}'_{m'})\boldsymbol{\phi}^T(\mathbf{x}'_{m'}) \\ \hat{\mathbf{h}} = \dfrac{1}{M}\displaystyle\sum_{n=1}^{N} \boldsymbol{\phi}(\mathbf{x}_{\boldsymbol{m}}). \end{cases} \tag{4.16}$$

Thus, the MSE is given by

$$J(\boldsymbol{\theta}) = \frac{1}{2}\boldsymbol{\theta}^T \hat{\mathbf{G}}\boldsymbol{\theta} - \boldsymbol{\theta}^T \hat{\mathbf{h}}. \tag{4.17}$$

The optimal vector, $\boldsymbol{\theta}_{\text{opt}}$, minimizes the above cost function. In order to avoid *overfitting*, an L_2 regularization is introduced to the cost function as

$$J'(\boldsymbol{\theta}) = \frac{1}{2}\boldsymbol{\theta}^T \hat{\mathbf{G}}\boldsymbol{\theta} - \boldsymbol{\theta}^T \hat{\mathbf{h}} + \frac{\lambda}{2}\|\boldsymbol{\theta}\|_2^2, \tag{4.18}$$

where λ is the regularization factor and $\|\mathbf{x}\|_2$ denotes the L_2 norm operation of a vector $\mathbf{x}$. Because this optimization is MMSE optimization, the optimal weighting vector satisfied $\dfrac{\partial J'(\boldsymbol{\theta})}{\partial \boldsymbol{\theta}} = 0$. The derivative of the cost function is

$$\frac{\partial J'(\boldsymbol{\theta})}{\partial \boldsymbol{\theta}} = \boldsymbol{\theta}^T \hat{\mathbf{G}} - \hat{\mathbf{h}}^T + \lambda\boldsymbol{\theta}^T. \tag{4.19}$$

From this, we can obtain optimal weighting vector as

$$\boldsymbol{\theta}_{\text{MMSE}} = (\hat{\mathbf{G}} + \lambda I_N)^{-1}\hat{\mathbf{h}}. \tag{4.20}$$

4.3.4 Anomaly Detection and Change Detection

The abnormal data detection is carried out based on the test data as follows:

1. Learning parameters are optimized from baseline samples and test samples.

2. Each test data are input to estimation model, and abnormality $a(x'_{n'})$ is calculated.
3. If this abnormality value is above threshold a_{th}, the input data is treated as abnormal data.

Moreover, abnormality detection of whole test data, i.e., detection of the distribution change change detection of distribution is available by taking above steps for each test data and taking sum of all outputted abnormality values.

Chapter 5

Proposed Scheme

5.1 Q-Learning Aided Resource Allocation

5.1.1 Design of Learning Model

Let *one epoch* be composed of the channel allocation, Q value observation, and learning process. The FC has one independent Q-learning equipment for each LoRaWAN node i.e., FC acts as an agent of Q-learning. The frequency channel assignment for the next epoch is determined based on the state at the current epoch. Without loss of generality, we explain the frequency channel assignment for LoRaWAN node n. Let us define state set $\mathcal{S}$, action set $\mathcal{A}$, and Q-value as below.

- State $\mathcal{S}$: the combination of the allocated channel indices of all the nodes. The frequency channel assignment for each LoRaWAN node is represented by one-hot-K vector, in which the element corresponding to the assigned frequency channel is set to 1, and otherwise set to 0. Thus, each state $S_t \in \mathcal{S}$ is a column vector by stacking up N one-hot-K vector. For example, suppose $N = 3$ and $K = 4$ and then one possible state is given by $(1, 0, 0, 0, 0, 1, 0, 0, 0, 1, 0, 0)$.

- Action $\mathcal{A}$: the set of channel indices which can be allocated to node n.

- Q-reward Q_{n,k_n}: the weighted sum of the number of received packets. It is adjusted by the ratio of the number of received packets from the node n of interest and the minimum number of received packets of other nodes, which is given as

$$Q_{n,k_n} = D_{n,t+1} + \nu \times \frac{\sum_{n' \in \mathcal{N} \setminus n} D_{n',t+1}}{N-1}, \tag{5.1}$$

where $D_{n,t}$ is the number of successfully received packets from LoRaWAN node n during epoch t, and ν is a $\mathit{selfish\ parameter}$ that adjusts priority between node n's reward and that of other nodes.

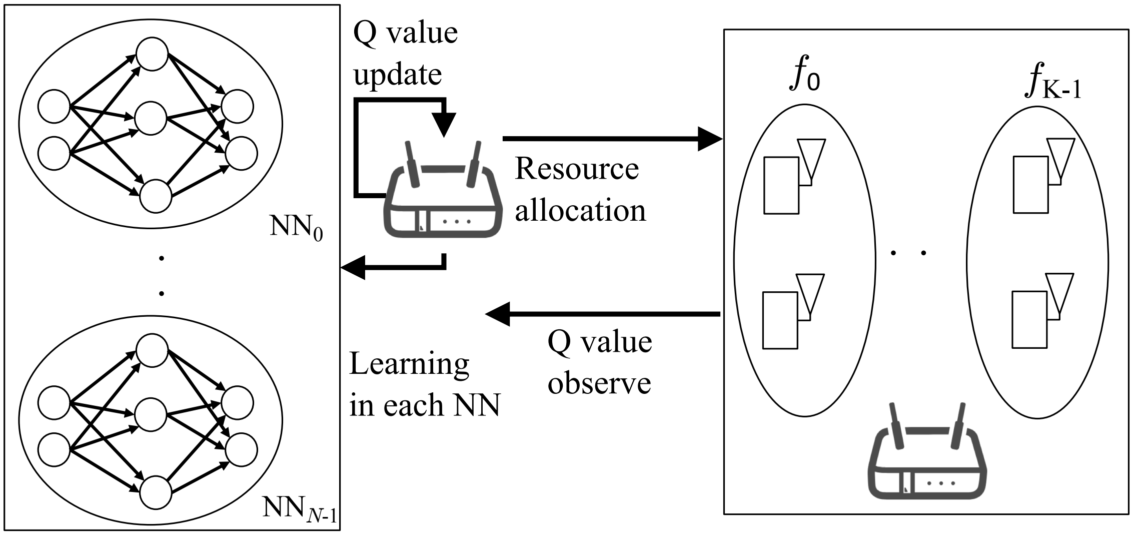

Figure 5.1: Proposed resource allocation model.

The selfish parameter ν is expressed as

$$\nu = \tanh\left(\frac{D_{n,t+1}}{\min_{n' \in \mathcal{N} \setminus n} D_{n',t+1}}\right). \tag{5.2}$$

When ν is small, node n acts selfishly and tries to increase its own number of received packets. On the other hand, if ν is large, FC attempts to equalize the performance of all nodes through resource allocation to node n.

This learning contains a two-step learning comprised of wireless environmental learning and optimal resource selection. The first part learns the wireless environment around each LoRaWAN node from the input channel allocation state. For example, this learning tries to understand which pair of LoRaWAN nodes do not interfere with each other even if they are allocated to the same frequency channel. The second part is the frequency channel allocation based on the wireless environment. Based on the learned wireless environment, the optimal frequency channel is assigned to each LoRaWAN node. In the proposed scheme, the two steps are connected and the frequency channel allocation is performed based on the input frequency channel allocation state.

5.1.2 Resource Allocation using Q-learning

The FC allocates one of K frequency channels to each LoRaWAN node based on the output from NN. The resource allocation at epoch t is performed as follows:

Step1 The agent inputs current resource allocation state S_t to the NN of each LoRaWAN node and obtains output Q-values $\{Q_{n,k_n}\}$ from each NN.

Step2 With probability $\epsilon(t)$, the FC randomly allocates one of K frequency channels to LoRaWAN node n. With probability $(\ 1 - \epsilon\ (t))$, the FC allocates frequency channel $k_n^\star$ to LoRaWAN node n, where $k_n^\star$ is given by

$$k_n^\star = \arg\max_{k_n \in \mathcal{K}} Q_{n,k_n}. \tag{5.3}$$

Step3 The FC observes the number of successfully received packets for state S_t.

By this, the FC can allocate the frequency channel that maximizes the number of successfully received packets having a correlation with the PDR to each LoRaWAN node.

5.2 Density Ratio Estimation based Interference Detection and Resource Reallocation

Fig. 5.2 shows the proposed model. The controller detects the inter-system interference state changes from the observable data at the FC using a distribution change detection scheme, e.g., density ratio estimation. In this letter, the controller splits observed data into two exclusive sets and generates two different distributions. The first distribution is generated from relatively old observed data, and the second distribution is generated from relatively new observed data. If these distributions are different, the controller decides that the interference state was changed. Although similar approaches are taken in the existing schemes [17, 18], these schemes assume interference state before observation, e.g., samples of distribution $p(x)$ are observed from the system without interference. No such assumption is required for the proposed scheme.

The proposed scheme has two advantages. First, it is not necessary to assume the interference state. Second, this scheme can detect the change of interference state, i.e., the appearance and the disappearance of the interference. This is because the proposed scheme does not assume the normal interference state.

5.2.1 Distribution Change Detection using Sliding Window

In this subsection, how to obtain the sample set from standard distribution $p(x)$ and that from test distribution $p'(x)$ is explained. The normalized number of successfully received packets $x_{k,t}^{\mathrm{smpl}}$ on frequency channel k during epoch t is used as a sample, which is obtained as

$$x_{k,t}^{\mathrm{smpl}} = \frac{\sum_{n \in N, k_n = k} D_{n,t+1}}{N_{k,t} \times T_{\mathrm{epoch}}}, \tag{5.4}$$

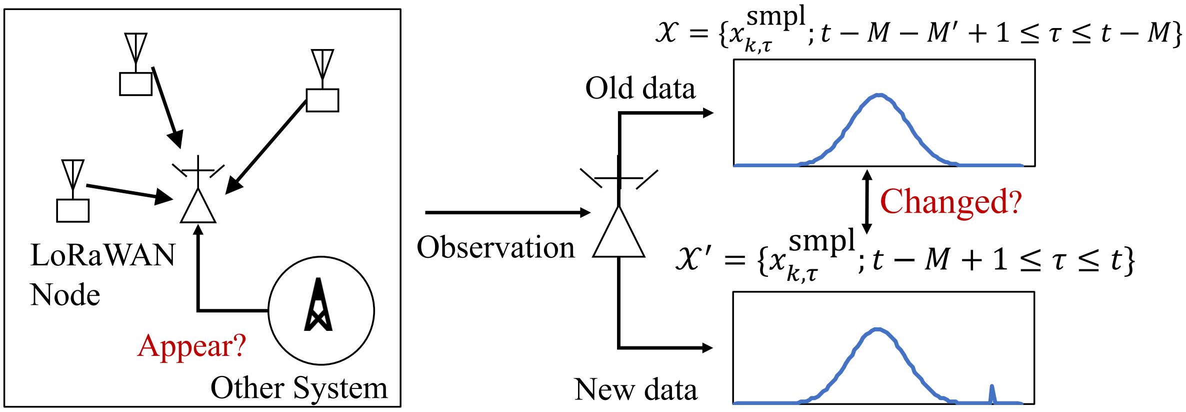
LoRaWAN Node
Appear?
Other System
Observation
$\mathcal{X} = \{x_{k,\tau}^{\text{smpl}}; t - M - M' + 1 \leq \tau \leq t - M\}$
Old data
Changed?
$\mathcal{X}' = \{x_{k,\tau}^{\text{smpl}}; t - M + 1 \leq \tau \leq t\}$
New data

Figure 5.2: Proposed interference detection model.

where $N_{k,t}$ is the number of LoRaWAN nodes allocated to frequency channel k during epoch t.

Let us denote the number of standard samples by M and that of test samples by M', and further let us define standard sample set $\mathcal{X} = (x_{k,t-M'-M}^{\text{smpl}}, \cdots, x_{k,t-M'-1}^{\text{smpl}})$ and test sample set $\mathcal{X}' = (x_{k,t-M'}^{\text{smpl}}, \cdots, x_{k,t-1}^{\text{smpl}})$ which are obtained as follows. Without loss of generality, let us consider the procedure at epoch t.

1. The observation data at epoch t, $x_{k,t-1}^{\text{smpl}}$, is obtained by (5.4).

2. Test sample set $\mathcal{X}'$ is updated as

$$\mathcal{X}' \leftarrow \mathcal{X}' \backslash x_{k,t-M'}^{\text{smpl}} \cup x_{k,t}^{\text{smpl}}.$$

3. Standard sample set $\mathcal{X}$ is updated as

$$\mathcal{X} \leftarrow \mathcal{X} \backslash x_{k,t-M'-M}^{\text{smpl}} \cup x_{k,t-M'}^{\text{smpl}}.$$

4. The density ratio, $r(\mathcal{X}, \mathcal{X}')$, is obtained as

$$r(\mathcal{X}, \mathcal{X}') = \frac{p(\mathcal{X}')}{p(\mathcal{X})},$$

where $p(\mathcal{X})$ is a function to generate a probability distribution function (PDF) from set $\mathcal{X}$.

5. If $r(\mathcal{X}, \mathcal{X}') > a_{\text{th}}$, then interference state is treated as changed.

The implementation example is shown in Fig. 5.3.

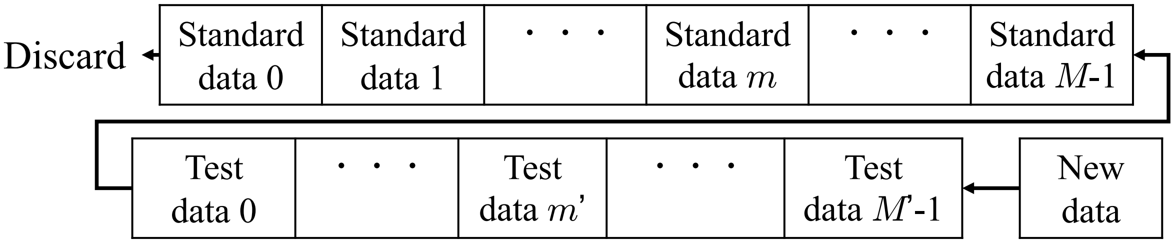

Figure 5.3: Generation of pseudo baseline sample and test sample.

5.2.2 ReLearning

Once the inter-system interference state is detected to be changed, the FC performs a Q-learning based wireless resource allocation proposed in previous section. Once the inter-system interference appears on a specific frequency channel, the system tries to avoid that frequency channel. On the other hand, once the inter-system interference disappears, the system tries to use the frequency channel previously contaminated by the inter-system interference.

Chapter 6

Performance Evaluation

In this section, we provide computer simulation results to verify the performance of the proposed scheme. In this simulation, the shadowing between the FC and each LoRaWAN node is calculated by a spatially correlated shadowing model [34]. This component is expressed as a function of the location of node $\psi(x_n, y_n)$. Between LoRaWAN nodes, shadowing is calculated using uncorrelated shadowing because the nodes are located near ground height, and shadowing correlation is very low due to the distance between nodes. Therefore, this component is expressed as the function of nodes index $\psi(n, q)$ where n and q are indices of nodes. In both, situations, uncorrelated shadowing is based on log-normally distributed shadowing loss with zero-mean and standard deviation of σ [dB].The wireless system parameters and traffic parameters are derived from Asian parameter configuration of LoRaWAN AS923 from document [2] and radio law of japan [6]. In this thesis, packet retransmission is not considered due to a limitation of downlink duty cycle [35]. Therefore, $CW = \mathrm{CW}_{\min}$ because $N_{r,n} = 0$. For learning parameters, we compare learning schemes and models e.g. the number of layers, learning rate, optimizers, etc. The optimal combination of learning parameters are used for PDR performance evaluation. In this thesis, we use RBF kernel that is

$$\phi_m(\mathbf{x}) = \exp(-\frac{\|\mathbf{x} - \mathbf{x}_m\|}{2h^2}). \tag{6.1}$$

Moreover, for the ϵ-greedy scheme, $\epsilon(t)$ is gicen as

$$\epsilon(t) = \frac{T - t}{T}, \tag{6.2}$$

where t is current epoch, and T is the number of epochs.

6.1 Performance Evaluation of Q-Learning Aided Resource Allocation

First, we evaluate performance of Q-learning resource allocation. In this section, we ignore inter-system interference, i.e., $P_{\mathrm{int},k} = -\infty\,[\mathrm{dBm}], \forall k$. For performance comparison, we also evaluate the perfor-

Table 6.1: Wireless system parameter

Simulation area $D \times D$	2×2 $[\mathrm{km}^2]$
Spreading factor SF	{7,8,9,10,11,12}
Bandwidth W	125 [kHz]
Duty cycle G	0.01
Transmit power P_{t}	13 [dBm]
Carrier frequency f_{c}	923 [MHz]
Number of LoRaWAN nodes N	5000
Propagation coefficient of distance loss a	4.0
Propagation offset b	9.5
Propagation coefficient of frequency loss c	4.5
Shadowing deviation σ	3.48 [dB]
Shadowing correlation coefficient	0.05
Noise power spectrum density	-174 [dBm/Hz]
Noise figure	9 [dB]
CS threshold Γ_{CS}	{-80, -90, -100, -110} [dB]
Number of frequency channels K	{2,4, 8,16}
Inter-system interference power $P_{\mathrm{int},k}$	$(-\infty, -\infty, -\infty, -93.0)$ [dBm]
Wi-SUN system state change time T_{int}	225 [epoch]

Table 6.2: Traffic parameter

Packet sizeN_{trans}	100 [bit]
Number of application types	2
Packet generation interval set $\mathcal{T}_{\mathrm{interval}}$	$\{60, 300\}$ [sec]
Probability of packet generation cluster	{0.5,0.5}
Event propagation speed	700 [m/sec]
Event propagation coefficient α	0.005

Table 6.3: Learning parameter

Optimizer	SGD [33]
activation function	ReLU
Length of one epoch for learning	600 [sec]
Number of epochs for learning T (initial, relearning)	(200,200)
Q-learning rate α	0.4
Number of NN layers L	$\{3, 4, 5\}$
Number of neurons of hidden layer	$\{10$ ($L = 3$), (10, 5) ($L = 4$), (10, 5, 5) ($L = 5$)$\}$
Learning rate	$\{10^{-1}, 10^{-2}, 10^{-3}, 10^{-4}\}$
hline Regularization parameter λ	0.001
RBF bandwidth h	0.001
change detection threshold a_{th}	10
The number of baseline sample M	5
The number of test sample M'	5

mance of conventional scheme. In the conventional scheme, each LoRaWAN node randomly selects one of frequency channels $\mathcal{K}$ at the start of each packet transmission.

6.1.1 Impacts of Learning Parameters

Number of Layers

It is well known that number of layers L has a strong impact on the output value of NN. Fig. 6.1 shows the impact of L on the PDR performance. As shown in Fig. 6.1, the optimal number of layers is 3. This because of the number of epochs. Training speed of NN depends on the number of layers. If the learning time is short, a small number of layers is better because NN can converge faster due to the small number of coupling weights. In the following section, $L = 3$ is used for NN.

Learning Rate

Next, the impact of the learning rate on the PDR is shown in Fig. 6.2. This result shows that learning rate $\eta = 10^{-3}$ gives the best PDR performance.

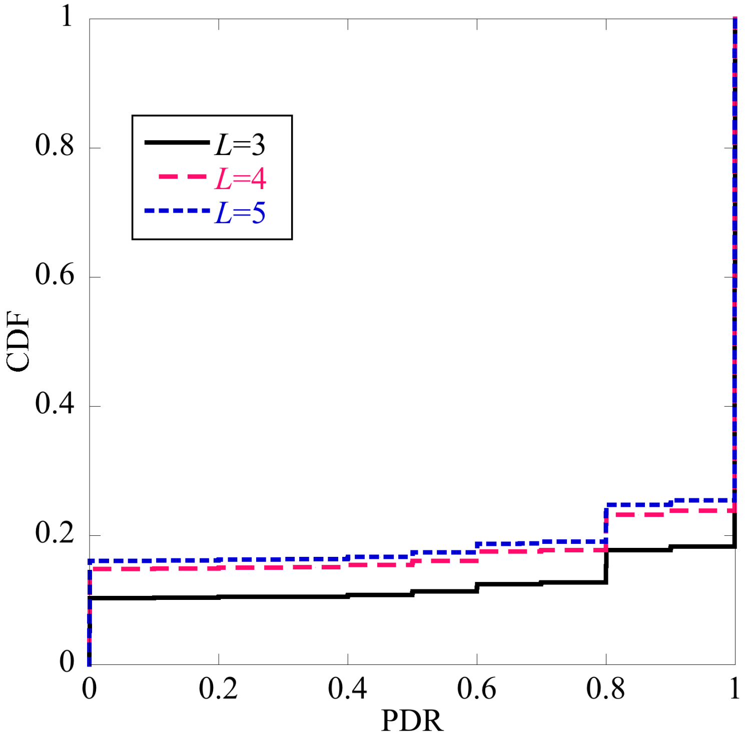

Figure 6.1: Impact of the number of layers, L.

6.1.2 PDR Performance

Fig. 6.3 shows how the learning proceeds. It can be seen from the figure that the PDR value improves as learning progresses. The impacts of number of frequency channels K and CS threshold Γ_{CS} on the PDR performance are shown in Fig. 6.4 and 6.5. Fig. 6.4 shows that the performance improvement from the proposed scheme depends on the number of available frequency channels, K. However the performance with lower PDR slightly degraded, the proposed scheme can improve the average PDR performance by about 13% when $K = 4$ compared with the conventional random allocation. However, the performance improvement becomes slightly smaller when $K = 8$ and $K = 16$. This is because the random channel hopping can avoid packet collision if the system has a sufficient number of channels. However, in a typical LoRaWAN system, only a small number of channels is available. For example, in the EU standard, the minimum number of channels is set to 3 [28]. Thus, it can be said that the proposed scheme is more effective in a practical environment.

Because the PDR performance of LoRaWAN with CSMA/CA highly depends on how accurately each LoRaWAN node can CS with each other, we evaluate the impact of the CS threshold Γ_{CS}. FIg. 6.5 shows that PDR performance of each Γ_{CS} does not change. It is because the proposed scheme allocate

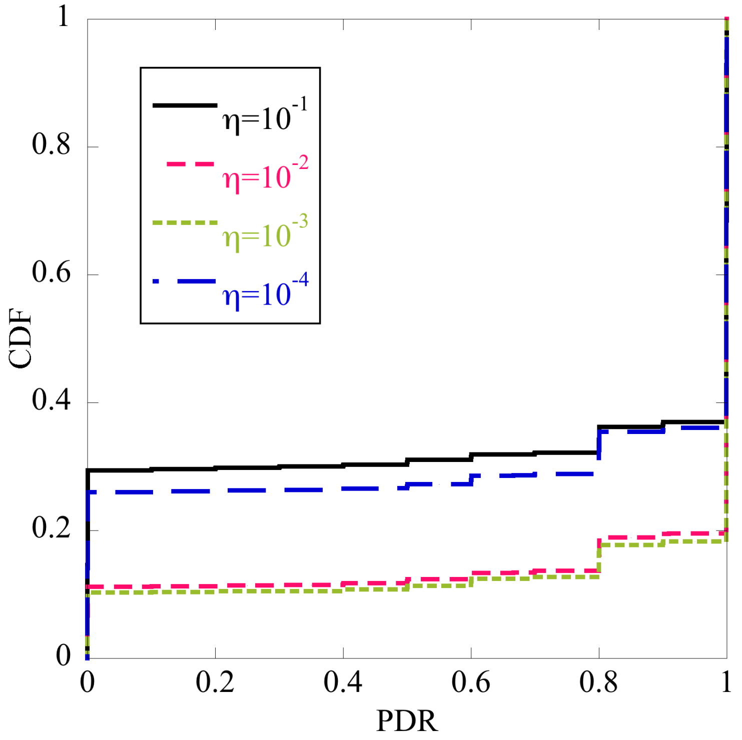

Figure 6.2: Impact of learning rate, η.

resource to avoid traffic collision with high priority.

6.2 Interference Detection and Resource Reallocation

Next, we evaluate interference detection accuracy and PDR performance for avoidance of inter-system interference. For performance comparison, we also evaluate the performance of the non-detection scheme. In the conventional scheme, FC does not detect inter-system interference. Therefore, system use the same allocated resource without taking into account of inter-system interference.

In this section, we evaluate performance of two cases, interference appearance and interference disappearance because the scope of this research is detection of both interference state change.

Interference appearance interference state is “disappear”at initial state and interference occur from T_{int}.

Interference disapperance interference state is “appear” at initial state and interference disappear from T_{int}.

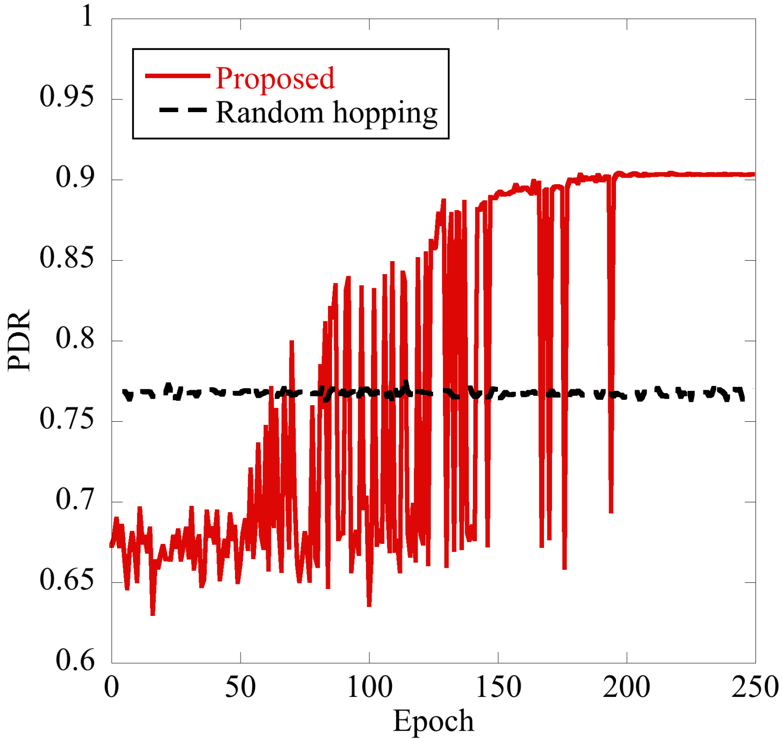

Figure 6.3: Learning process.

6.2.1 Case 1: Interference Appearance

In this scenario, the interference state is initially "disappearance", and the interference appears at T_{int}. Fig. 6.6 shows how the proposed interference detection scheme can detect the change of the interference status. It can be seen from the figure that the PDR performance severely degrades if no interference detection is introduced. By introducing the proposed interference detection scheme, the system can successfully detect the change of the interference state and execute the relearning process. Thus, it can significantly improve the PDR performance. Although it takes additional learning overhead, the proposed scheme can efficiently allocate the frequency channels by avoiding the frequency channel contaminated by the inter-system interference. This performance improvement is also clear in Fig. 6.7, where the cumulative distribution function (CDF) of PDR is shown. In this scenario, the proposed scheme can improve the average PDR performance by about 10%.

6.2.2 Case 2: Interference Disappearance

In this scenario, the interference state is initially "appearance", and the interference appears at T_{int}. Fig. 6.8 shows how the interference detection scheme can also detect the disappearance of the interference

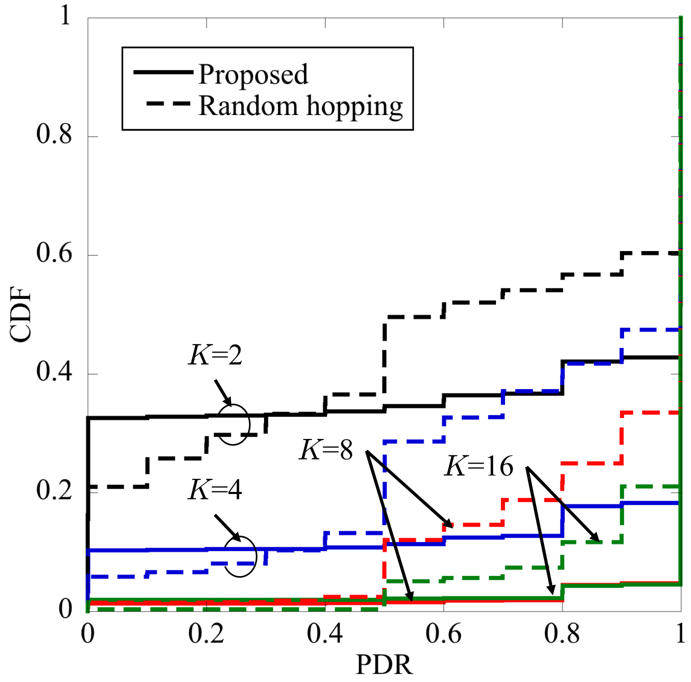

Figure 6.4: Impact of the number of resources, K.

status. It can be seen from the figure that the PDR performance slightly improves if no interference detection is introduced. The available frequency resources are not efficiently utilized. By introducing the proposed interference detection scheme, the system can successfully detect the change of the interference state and execute the relearning process. Thus, it can significantly improve the PDR performance. Although it takes additional learning overhead, the proposed scheme can efficiently utilize the frequency channel previously contaminated by the inter-system interference. This performance improvement is also shown in Fig. 6.9. In this situation, the proposed scheme can improve the average PDR performance by about 8%.

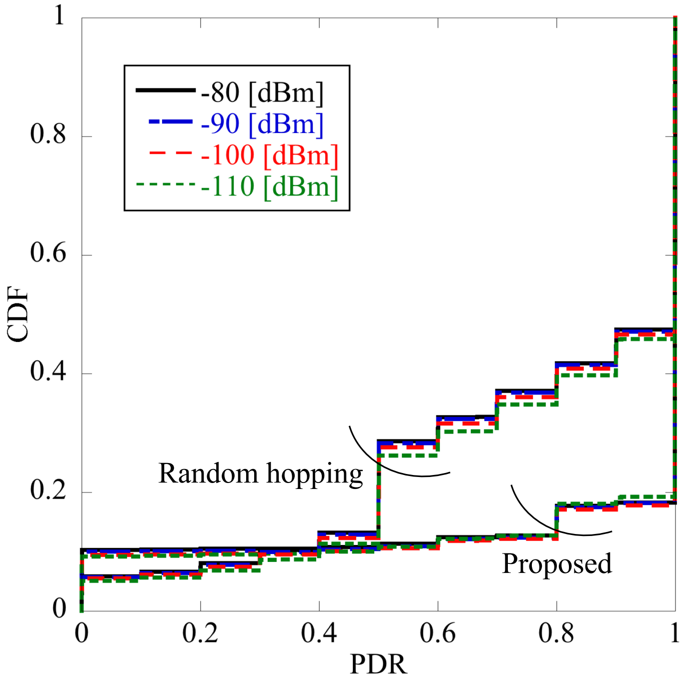

Figure 6.5: Impact of CS threshold, Γ_{CS}.

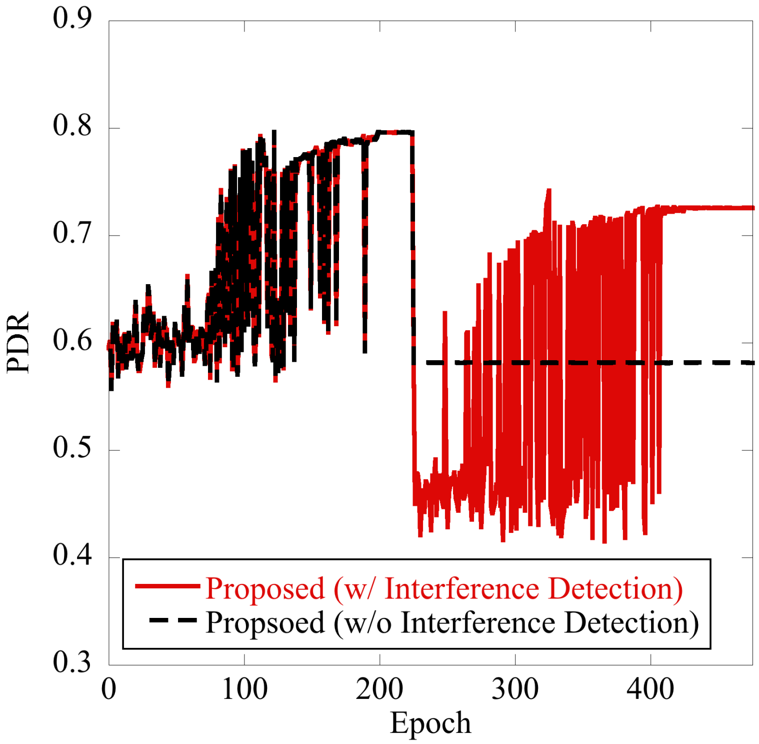

Figure 6.6: Learning process with appeared interference.

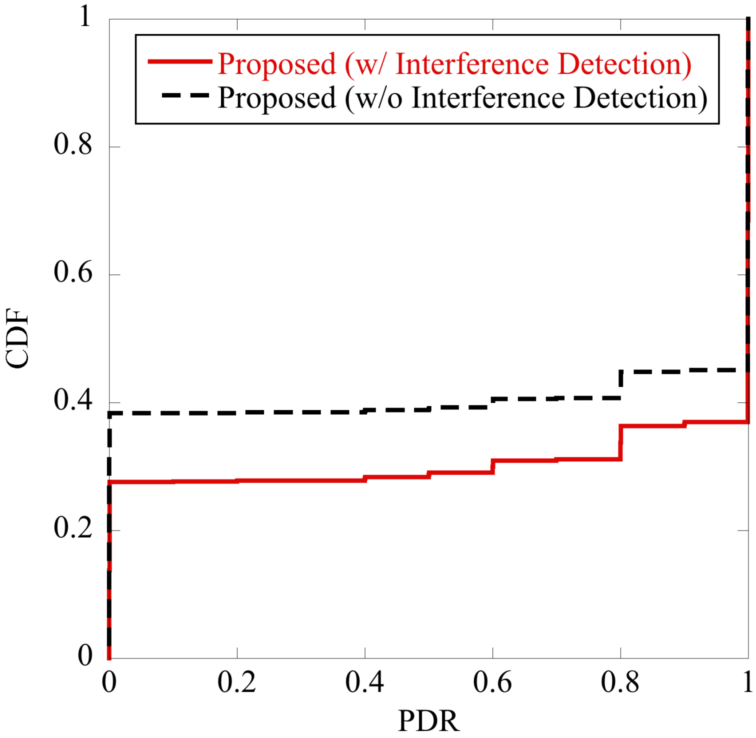

Figure 6.7: CDF of PDR with appeared interference.

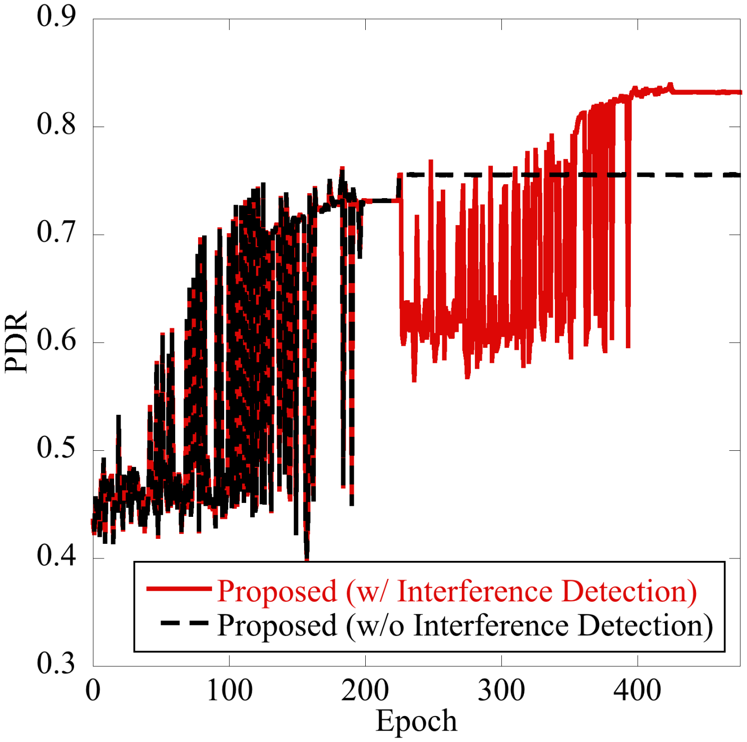

Figure 6.8: Learning process with disappeared interference.

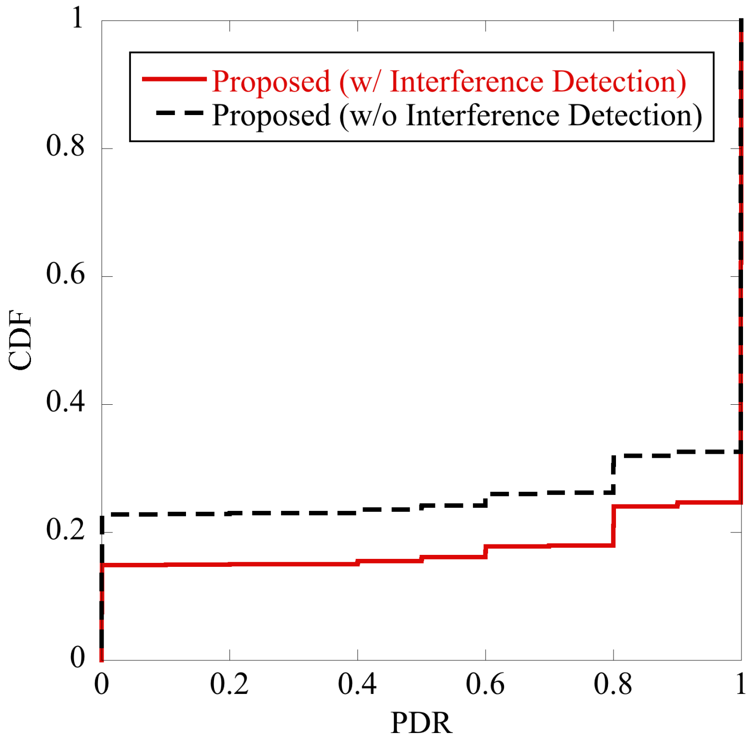

Figure 6.9: CDF of PDR with disappeared interference.

Chapter 7

Conclusion

In this thesis, we tackled the orthogonal frequency channel allocation in LoRaWAN. The proposed scheme adopts reinforcement learning and NN approximation. This scheme utilizes the weighted sum of the number of successfully received packets from each LoRaWAN node as a reward. Thus, it does not require any explicit feedback from LoRaWAN nodes. Searching for the optimal frequency allocation that maximizes the reward, each node can avoid packet collision. Furthermore, we have proposed a detection scheme of the interference state to enable efficient frequency channel allocation. This detection scheme estimates the interference state based on the density ratio estimation and baseline data generation using a sliding window. Thus, FC can detect the change of interference state without any prior assumption and knowledge. The extensive computer simulation results show that the proposed scheme can improve the average PDR performance by about 17%. Moreover, it is shown that the proposed scheme can detect the change of interference state at most 3 observations and can improve average PDR performance by about 10% compared to the system without the detection of the interference state. These results indicate that the proposed scheme could improve PDR performance without preparing more wireless resources and explicit feedback that drain LoRaWAN batteries.

Acknowledgment

In promoting this resource and preparation of this thesis, I would like to express great thanks to my supervisor, associate Prof. Adachi. Furthermore, I would also like to thank Prof. Yamao, Prof. Fujii, and associate Prof. Ishibashi for meaningful discussions and advice on the research contents. I would also like to thank associate Prof. Takyu in Shinshu Univ. and assistant Prof. Ohta in Fukuoka Univ. for insightful comment in my research. Also, thank you for the continuous support of AWCC members and my family.

References

[1] U. Raza, P. Kulkarni, and M. Sooriyabandara, “Low Power Wide Area Networks: An Overview,” *IEEE Commun. Surveys & Tut.*, vol. 19, no. 2, pp. 855–873, 2017.

[2] LoRa Alliance Technical Commitee, “LoRaWAN 1.1 Specification,” 2017. [Online]. Available: https://lora-alliance.org/resource-hub/lorawantm-specification-v11

[3] T. Deng, J. Zhu, and Z. Nie, “An Improved LoRaWAN Protocol Based on Adaptive Duty Cycle,” in *Proc. IEEE Inform. Technol. and Mechatronics Eng. Conf.*, 2017, pp. 1122–1125.

[4] J. Ortin, M. Cesana, and A. Redondi, “How do ALOHA and Listen Before Talk Coexist in LoRaWAN ?” in *Proc. IEEE Int. Symp. on Personal, Indoor and Mobile Radio Commun.*, 2018, pp. 1–7.

[5] ——, “Augmenting LoRaWAN Performance with Listen Before Talk,” *IEEE Trans. on Wireless Commun.*, vol. 18, no. 6, pp. 3113–3128, 2019.

[6] ARIB, “920MHz-BAND TELEMETER, TELECONTROL AND DATA TRANSMISSION RADIO EQUIPMENT,” 2012. [Online]. Available: http://www.arib.or.jp/english/html/overview/doc/5-STD-T108v1_2-E3.pdf

[7] J. T. Lim and Y. Han, “Spreading Factor Allocation for Massive Connectivity in LoRa Systems,” *IEEE Commun. Lett.*, vol. 22, no. 4, pp. 800–803, 2018.

[8] M. El-Aasser, T. Elshabrawy, and M. Ashour, “Joint Spreading Factor and Coding Rate Assignment in LoRaWAN Networks,” in *Proc. IEEE Global Conf. on Internet of Things*, 2019, pp. 1–7.

[9] L. Amichi, M. Kaneko, N. E. Rachkidy, and A. Guitton, “Spreading Factor Allocation Strategy for LoRa Networks under Imperfect Orthogonality,” in *Proc. IEEE Int. Conf. on Commun.*, 2019, pp. 1–7.

[10] F. Cuomo, M. Campo, A. Caponi, G. Bianchi, G. Rossini, and P. Pisani, "EXPLoRa: Extending the Performance of LoRa by Suitable Spreading Factor Allocations," in *Proc. Int. Conf. on Wireless and Mobile Comput., Networking and Commun.*, 2017.

[11] A. Waret, M. Kaneko, A. Guitton, and N. El Rachkidy, "LoRa Throughput Analysis with Imperfect Spreading Factor Orthogonality," *IEEE Wireless Commun. Lett.*, vol. 8, no. 2, pp. 408–411, 2019.

[12] A. Tiurlikova, N. Stepanov, and K. Mikhaylov, "Method of Assigning Spreading Factor to Improve the Scalability of the LoRaWan Wide Area Network," in *Proc. Int. Congress on Ultra Modern Telecommun. and Control Syst. and Workshops*, vol. 2018-Novem. IEEE, 2019, pp. 1–4.

[13] C. Orfanidis, L. M. Feeney, M. Jacobsson, and P. Gunningberg, "Investigating Interference Between LoRa and IEEE 802.15.4g Networks," in *Proc. Int. Conf. on Wireless and Mobile Comput., Networking and Commun.*, 2017, pp. 1–8.

[14] A. J. Coulson, "Spectrum Sensing Using Hidden Markov Modeling," in *Proc. IEEE Int. Conf. on Commun.*, 2009, pp. 1–6.

[15] A. Badawy, A. E. Shafie, and T. Khattab, "On the Performance of Quickest Detection Spectrum Sensing: The Case of Cumulative Sum," *Arxiv*, pp. 1–5, 2020. [Online]. Available: http://arxiv.org/abs/2001.07828

[16] K. Wu, H. Tan, H. L. Ngan, Y. Liu, and L. M. Ni, "Chip Error Pattern Analysis in IEEE 802.15.4," *IEEE Trans. on Mobile Comput.*, vol. 11, no. 4, pp. 543–552, 2012.

[17] F. Barac, S. Caiola, M. Gidlund, E. Sisinni, and T. Zhang, "Channel Diagnostics for Wireless Sensor Networks in Harsh Industrial Environments," *IEEE Sensors J.*, vol. 14, no. 11, pp. 3983–3995, 2014.

[18] C. H. Uy, C. Bernier, and S. Charbonnier, "Design of a Low Complexity Interference Detector for LPWA Networks," in *Proc IEEE Int. Instrumentation and Measurement Technol. Conf.*, 2019, pp. 1–6.

[19] J. Liu, R. Deng, S. Zhou, and Z. Niu, "Seeing the Unobservable: Channel Learning for Wireless Communication Networks," in *Proc. IEEE Global Commun. Conf.*, 2015, pp. 1–6.

[20] S. Chen, Z. Jiang, J. Liu, R. Vannithamby, S. Zhou, Z. Niu, and Y. Wu, "Remote Channel Inference for Beamforming in Ultra-Dense Hyper-Cellular Network," in *Proc. IEEE Global Commun. Conf.*, 2017, pp. 1–6.

[21] F. Meng, P. Chen, and L. Wu, "Power Allocation in Multi-User Cellular Networks with Deep Q Learning Approach," in *Proc. IEEE Int. Conf. on Commun.*, 2019, pp. 1–6.

[22] K. Nakashima, S. Kamiya, K. Ohtsu, K. Yamamoto, T. Nishio, and M. Morikura, "Deep Reinforcement Learning-Based Channel Allocation for Wireless LANs with Graph Convolutional Networks," in *Proc. IEEE Veh. Technol. Conf.*, 2019, pp. 1–5.

[23] H. Ye, L. Liang, G. Y. Li, and B.-H. F. Juang, "Deep Learning based End-to-End Wireless Communication Systems with Conditional GAN as Unknown Channel," in *Proc. IEEE Global Commun. Conf. Workshops*, 2019, pp. 1–5.

[24] V. Mnih, K. Kavukcuoglu, D. Silver, A. A. Rusu, J. Veness, M. G. Bellemare, A. Graves, M. Riedmiller, A. K. Fidjeland, G. Ostrovski, S. Petersen, C. Beattie, A. Sadik, I. Antonoglou, H. King, D. Kumaran, D. Wierstra, S. Legg, and D. Hassabis, "Human-Level Control Through Deep Reinforcement Learning," *Nature*, vol. 518, no. 7540, pp. 529–33, 2015.

[25] T. Kanamori, S. Hido, and M. Sugiyama, "A Least-Squares Approach to Direct Importance Estimation," *J. of Machine Learning Research*, vol. 10, pp. 1391–1445, 2009.

[26] LoRa Alliance Technical Committee, "LoRaWAN Regional Parameters v1.1 REV B," 2018. [Online]. Available: https://lora-alliance.org/resource-hub/lorawanr-regional-parameters-v11rb

[27] Semtech Corporation, "LoRa Modem Design Guide SX1272/3/6/7/8." p. 9, 2013. [Online]. Available: https://www.semtech.com/uploads/documents/LoraDesignGuide_STD.pdf

[28] V. Gupta, S. K. Devar, N. H. Kumar, and K. P. Bagadi, "Modelling of IoT Traffic and Its Impact on LoRaWAN," in *Proc. IEEE Global Commun. Conf.*, 2017, pp. 1–6.

[29] C. Goursaud and J. M. Gorce, "Dedicated Networks for IoT: PHY / MAC State of The Art and Challenges," *EAI Endorsed Trans. on Internet of Things*, vol. 1, no. 1, p. 150597, 2015.

[30] D. Croce, M. Gucciardo, S. Mangione, G. Santaromita, and I. Tinnirello, "Impact of LoRa Imperfect Orthogonality : Analysis of Link-Level Performance," *IEEE Commun. Lett.*, vol. 22, no. 4, pp. 796–799, 2018.

[31] R. S. Sutton and A. G. Barto, *Reinforcement Learning: An Introduction, by Sutton, R.S. and Barto, A.G.* The MIT Press, 1999, vol. 3, no. 9. [Online]. Available: http://linkinghub.elsevier.com/retrieve/pii/S1364661399013315

[32] C. M. Bishop, *Pattern Recognition and Machine Learning*. Springer, 2010.

[33] N. Buduma and N. Locascio, *Fundamentals of Deep Learning*. o'reilly, 2017.

[34] H. Claussen, "Efficient Modelling of Channel Maps with Correlated Shadow Fading in Mobile Radio Systems," in *Proc. IEEE Int. Symp. on Personal, Indoor and Mobile Radio Commun.*, 2005, pp. 512–516.

[35] V. D. I. Vincenzo, M. Heusse, L. I. G. Cnrs, and B. Tourancheau, “Improving Downlink Scalability in LoRaWAN,” in *Proc. IEEE Int. Conf. on Commun.*, 2019.

Publication

i. N. Aihara, K. Adachi, O. Takyu, M. Ohta, T. Fujii, “Q-Learning Aided Resource Allocation and Environment Recognition in LoRaWAN with CSMA/CA,” *IEEE Access*, vol. 7, no. 1, pp. 152126-152137, 2019.

ii. N. Aihara and K. Adachi, “Orthogonal Resource Allocation Using SVM for CSMA/CA,” *in Proc. Asia-Pacific Signal and Inform. Processing Association Annual Summit and Conf.*, pp. 779-784, Hawaii, 12-15, Nov. 2018.

iii. M. Ohta, K. Adachi, N. Aihara, O. Takyu, and T. Fujii, M. Taromaru, “Measurement experiments on 920 MHz Band for Spectrum Sharing with LoRaWAN,”*in Proc. IEEE Veh. Technol. Conf. ’18-fall*, 2018, pp. 1-6, Chicago, 27-30, Aug. 2018.

iv. Chaleunsouk Bounpasith, 相原 直紀，安達 宏一，“他システムへの干渉を考慮したLoRaWANの送信制御法の検討,” 信学総大, B-5-167, 2020年3月

v. 蕪木 碧仁, 相原 直紀, 安達 宏一, 田久 修, 太田 真衣, 藤井 威生, “IoTにおける送信タイミングの自律分散的制御法の検討,” 信学総大, B-5-121, 2020年3月

vi. 相原　直紀, 安達宏一, 田久修, 太田真衣, 藤井威生, “LoRaWANにおける外部干渉検知システムにおける学習パラメータ再初期化,” 信学総大, B-5-122, 2020年3月

vii. 相原 直紀, 安達宏一, 田久修, 太田真衣, 藤井威生, “LoRaWANにおける教師なし外部検出手法及び無線リソース再割り当て手法,” 信学技報, vol. 119, no. 378, RCS2019-275, pp. 57-62, 2020年1月.

viii. 相原 直紀, 安達 宏一, 田久 修, 太田 真衣, 藤井 威生, “LoRaWANにおける強化学習を用いた周波数チャネル割り当て手法,” IEICE超知性ネットワーキングに関する分野横断型研究会（RISING 2019）, 2019年11月．**（RISING2019優秀ポスター発表賞受賞）**

ix. N. Aihara, K. Adachi, T. Osamu, M. Ohta, and T. Fujii, “[Poster Presentation] Reinforcement Learning Aided Orthogonal Frequency Allocation in LoRaWAN,” IEICE Smartcom 2019, vol. 119, no.262, SR2019-81, pp. 45-46, New Jersy, USA, Nov. 2019

x. 相原直紀, 安達宏一, 田久修, 太田真衣, 藤井威生, “LoRaWANにおける深層強化学習を用いた直交リソース割り当て法における報酬値の影響に関する検討,” 信学ソ大, B-5-80, 2019年9月.

xi. 相原直紀, 安達宏一, 田久修, 太田真衣, 藤井威生, “ニューラルネットワークに基づくQ学習を用いた無線リソース割り当て手法,” 信学技報, vol. 118, no. 435, RCS2018-261, pp. 109-114, 2019年1月. **（RCS研究会初年度発表者コンペティション優秀賞受賞）**

xii. N. Aihara, K. Adachi, O. Takyu, M. Ohta, and T. Fujii, “[Poster Presentation] SVM Based Orthogonal Resource Allocation in CSMA/CA,” IEICE SmartCom 2018, vol. 118, no. 274, SR2018-82, pp. 57-58, Bangkok, Thailand, Oct. 2018.

xiii. 相原直紀, 安達宏一, 田久修, 太田真衣, 藤井威生, “機械学習を用いる無線リソース割り当て法に関する一検討,” 信学技報, vol. 118, no. 12, RCS2018-21, pp. 109-114, 2018年4月.